


RESEARCH

Open Access



# Insights into the genome and secretome of *Fusarium metavorans* DSM105788 by cultivation on agro-residual biomass and synthetic nutrient sources

Sophie C. Brandt<sup>1†</sup>, Hévila Brognaro<sup>2,3†</sup>, Arslan Ali<sup>3,4,5</sup>, Bernhard Ellinger<sup>6</sup>, Katharina Maibach<sup>7</sup>, Martin Rühl<sup>8</sup>, Carsten Wrenger<sup>2,3</sup>, Hartmut Schlüter<sup>3,5</sup>, Wilhelm Schäfer<sup>1</sup>, Christian Betzel<sup>3</sup>, Stefan Janssen<sup>7</sup> and Martin Gand<sup>1,8\*</sup> 

## Abstract

**Background:** The transition to a biobased economy involving the depolymerization and fermentation of renewable agro-industrial sources is a challenge that can only be met by achieving the efficient hydrolysis of biomass to mono-saccharides. In nature, lignocellulosic biomass is mainly decomposed by fungi. We recently identified six efficient cellulose degraders by screening fungi from Vietnam.

**Results:** We characterized a high-performance cellulase-producing strain, with an activity of 0.06 U/mg, which was identified as a member of the *Fusarium solani* species complex linkage 6 (*Fusarium metavorans*), isolated from mangrove wood (FW16.1, deposited as DSM105788). The genome, representing nine potential chromosomes, was sequenced using PacBio and Illumina technology. In-depth secretome analysis using six different synthetic and artificial cellulose substrates and two agro-industrial waste products identified 500 proteins, including 135 enzymes assigned to five different carbohydrate-active enzyme (CAZyme) classes. The *F. metavorans* enzyme cocktail was tested for saccharification activity on pre-treated sugarcane bagasse, as well as untreated sugarcane bagasse and maize leaves, where it was complemented with the commercial enzyme mixture Accellerase 1500. In the untreated sugarcane bagasse and maize leaves, initial cell wall degradation was observed in the presence of at least 196 µg/mL of the in-house cocktail. Increasing the dose to 336 µg/mL facilitated the saccharification of untreated sugarcane biomass, but had no further effect on the pre-treated biomass.

**Conclusion:** Our results show that *F. metavorans* DSM105788 is a promising alternative pre-treatment for the degradation of agro-industrial lignocellulosic materials. The enzyme cocktail promotes the debranching of biopolymers surrounding the cellulose fibers and releases reduced sugars without process disadvantages or loss of carbohydrates.

**Keywords:** *Fusarium solani* species complex, *Fusarium metavorans*, Genome analysis, Secretome, Mass spectrometry, Proteomics, CAZyme analysis, Cellulose degradation, Residual biomass treatment

\*Correspondence: martin.gand@lcb.chemie.uni-giessen.de

<sup>†</sup>Sophie C. Brandt and Hévila Brognaro contributed equally to this work

<sup>1</sup> Faculty of Mathematics, Computer Science and Natural Science, Department of Biology, Biozentrum Klein Flottbek, Molecular Phytopathology, University of Hamburg, Ohnhorststr. 18, 22609 Hamburg, Germany

Full list of author information is available at the end of the article

## Background

Lignocellulosic biomass is the only sustainable source of organic carbon, offering a promising resource for the production of fuels, chemicals and carbon-based materials [1]. However, the use of lignocellulosic biomass must



be considered in the context of sustainable agriculture to avoid competition with food and feed production [2]. Biotechnological approaches are therefore required to valorize non-edible biomass, focusing on abundant sources such as forestry and agricultural wastes [3]. Sugarcane is the dominant crop in tropical areas such as South America and South Asia [4], whereas maize dominates in sub-tropical and temperate regions such as North America and Northern Europe [5]. The widespread agricultural use of these two C4 crops generates large quantities of lignocellulosic biomass that can be valorized without compromising food/feed production.

Lignocellulosic biomass has a heterogeneous structure and composition dependent on the plant species [6–8]. The main component is cellulose, the most abundant polymer on earth, consisting of linear chains of several hundred to many thousand  $\beta$ -(1,4)-D-glucose units. The other components are hemicellulose, pectin, lignin and extractives, the latter comprising a diverse range of substances that impede the enzymatic hydrolysis of biomass [9, 10]. Hemicellulose, the second most abundant polymer in plant cell walls [11], features at least six different macromolecules with varying ratios of pentose (xylose and arabinose) and hexose (mostly mannose and glucose) residues [12]. Xylans have a linear backbone of  $\beta$ -(1,4)-linked  $\beta$ -D-xylopyranosyl residues, whereas glucuronoxylans feature substituted 4-O-methyl- $\alpha$ -D-glucuronopyranosyl units and acetyl groups, and arabinoxylans contain xylose substituted with  $\alpha$ -L-arabinofuranosyl units [11]. Xyloglucans have a cellulose-like linear backbone of  $\beta$ -(1,4)-D-glucose with additional  $\beta$ -(1,6)-linked xylose sidechains, often capped with galactose and fucose [13]. Glucomannans have backbones of  $\beta$ -(1,4)-linked D-mannose and D-glucose, sometimes with branching  $\beta$ -(1,6)-glucosyl residues [14], but if  $\alpha$ -(1,6)-linked galactose units are present the polymers are known as galactoglucomannans [15]. Pectin is a complex heteropolymer of covalently linked D-galacturonic acid and other residues, and is also a significant component of sugarcane and maize bagasse [16]. The main constituents are (1) homogalacturonan, comprising linear  $\alpha$ -(1,4)-D-galactouronic acid chains with some esterified or O-acetylated modifications; (2) rhamnogalacturonan-I, comprising repeated disaccharides of galacturonic acid and C-3 or C-2 O-acetylated rhamnosyl residues, with linear or branched  $\alpha$ -L-arabinofuranosyl and/or galactopyranosyl side chains on C-4; and (3) substituted galacturonans as linear and side chain residues (rhamnogalacturonan-II), resulting in 12 types of glycosyl units that form at least 22 types of glycosidic bonds [17].

The recalcitrance of lignocellulosic biomass in part reflects the complexity of the substrate, with complete hydrolysis requiring efficient enzymes for the digestion

of cellulose as well as palettes of enzymes that can digest the components of hemicellulose [18] and pectin [19]. However, enzymatic hydrolysis is also impeded by the inaccessibility of the substrates, which can be addressed by physical and/or chemical pre-treatment. Such processes can generate inhibitors that limit the activity of cellulases and other enzymes, as well as toxic molecules such as furfurals, acetic acid, formic acid and lignin-derived phenolic compounds that interfere with fermentation [20]. The effect of biomass pre-treatment [21, 22] can therefore be improved by optimizing the enzymatic cocktails used to hydrolyze lignocellulosic biomass, tailoring them for the type of biomass and for the ability to tolerate inhibitors [1, 9, 10, 23]. Although the polysaccharide content of maize leaf and sugarcane culm cell walls is similar [24, 25], the cross-linking of polysaccharides and the interactions between polysaccharide and lignin/phenolic compounds differ, resulting in unique cell wall architectures. The physical and chemical characteristics of the biomass therefore reflect variations in the degree of cellulose polymerization, crystallinity, and lignin content, the hemicellulose and pectin content, and cell wall thickness [26].

Lignocellulosic biomass in nature is mainly decomposed by fungi, which are therefore promising candidates for the discovery of enzymes or enzyme cocktails for biomass degradation [27]. More than 5 million species of fungi have been described, and the number is likely to increase given that only 5% of species are formally classified [28, 29]. The subkingdom Dikarya consists of two phyla: Ascomycota, the largest phylum, commonly known as sac fungi [30], and Basidiomycota, the second largest phylum, commonly known as higher mushrooms or pillar fungi. The filamentous ascomycetes are ubiquitous and *Fusarium* is one of the most abundant genera in that phylum [31]. *Fusarium* species are frequently isolated from tropical, sub-tropical, and temperate environments, and less frequently from alpine habitats [32]. The genus *Fusarium* was first described at the beginning of the nineteenth century [33, 34]. Nine species have been described, including the easily recognized *Fusarium solani*, based on its striking morphology [35]. However, the current concept of *F. solani* is a species complex (FSSC) within the class Sordariomycetes, order Hypocreales, and the family Nectriaceae. The FSSC is thought to contain at least 60 phylogenetically distinct but closely related and morphologically similar species [36], and is allied with the sexual species *Nectria haematococca*. Robust classification within the FSSC and the genus *Fusarium* is achieved by analyzing polymorphisms in the genes encoding translation elongation factor 1 $\alpha$  (TEF1) and the second largest subunit of RNA polymerase II (RPB2) as well as the internal transcribed spacer

(ITS) together with 28S ribosomal RNA (ITS + 28S) [36–38]. Members of the FSSC collectively have a broad host range and can be found as soil-dwelling saprophytes, rhizosphere colonizers, or pathogens of pea, bean, potato, soybean, maize and many cucurbit plants, as well as animals including humans [39]. *Fusarium* sp. of the FSSC has 5–17 chromosomes, with a genome size of 40–54 Mbp and a GC content of ~50% [35, 40–42].

Our previously reported analysis of 295 fungal isolates, collected from different substrates and various environments in Vietnam, revealed their ability to degrade lipids, chitin, cellulose and xylan [43]. Six isolates were able to digest carboxymethylcellulose (CMC) with remarkable efficiency, two of which were *Fusarium* strains. We selected the most active member of FSSC linkage 6, isolated from dead mangrove wood, for further analysis. We characterized this strain as *F. metavorans* FW16.1 by analyzing its genome and secretome, leading to the identification of undiscovered lignocellulose degrading enzymes with the ability to convert sugarcane bagasse and maize leaves into fermentable sugars.

## Results

### Characterization, genomic analysis and phylogenetics of *F. metavorans* FW16.1

We tested the carboxymethylcellulase (CMCase) activity of *F. metavorans* FW16.1 on media containing 1% CMC 3 days after inoculation, revealing a value of  $0.055 \pm 0.001$  U/mg (Additional file 1: Table S1). Genomic DNA was isolated and analyzed by agarose gel electrophoresis (Additional file 1: Fig. S1) and the ITS region was amplified and sequenced (Additional file 1: Supplementary Data). Sequencing identified the isolate as a *F. solani* strain in the FSSC. The strain is preserved at the German Collection of Microorganisms and Cell Cultures (DSMZ) under the identifier DSM105788. The assembled FW16.1 genome was 48.28 Mbp in length, distributed over nine scaffolds with a GC content of 50.83% and an  $N_{50}$  scaffold length (weighted median of a contig length needed to cover 50% of the genome) of 6.66 Mbp. The optimal  $k$ -mer length (subsequences of length  $k$  contained in genomic sequence) following assembly with SOAPdenovo was  $k = 15$  bp, with a  $pkdepth$  (peak depth estimated from  $k$ -mer distribution) of 30. Gene prediction revealed the presence of 15,626 putative open reading frames (ORFs) with an average of 1618.9 bp per gene or 1459.85 bp per coding sequence. The whole genome is available as a biosample from the National Center for Biotechnology Information (NCBI) under the bioproject PRJN413482, accession number JADNRB000000000. Phylogenetic analysis assigned FW16.1 to the FSSC 6 linkage, with highest similarity to *F. metavorans* NRRL

43489 (Fig. 1). Growth on six different media resulted in the formation of pale mycelia (Fig. 2).

### Carbohydrate-active enzyme analysis

The FW16.1 genomic regions marked as protein coding sequences (CDS) in our de novo assembly were searched for homologs of families (and subfamilies) in the CAZyme database representing enzymes involved in cellulose and sugar metabolism, revealing 694 putative genes (Fig. 3; Table 1). The candidates were assigned to five different carbohydrate-active enzyme (CAZyme) classes, which were divided into their families (Additional file 1: Table S2).

### Evaluation of enzymatic activity

FW16.1 was cultivated in liquid yeast extract peptone dextrose (YPD) medium, and the enzymatic activity of the supernatant was tested. We observed CMCase activity that increased over the first 2 days, reaching a plateau of  $\sim 19.5 \pm 0.3$  U/mg that lasted until day 5. A further increase in activity on days 6 and 7 led to a new plateau at  $\sim 30$  U/mg (Additional file 1: Fig. S2). We then measured enzyme activity induced by cultivation in a range of liquid media containing synthetic and artificial cellulose substrates for 72 h. The activity of the FW16.1 supernatant was  $0.039 \pm 0.001$  U/mg against the crystalline cellulose Avicel PH-101 (Additional file 1: Fig. S3), increasing to  $0.07 \pm 0.01$  U/mg against  $\alpha$ -cellulose, and  $0.18 \pm 0.06$  U/mg against hydroxyethylcellulose (HEC). The specific activity against high, medium and low-viscosity forms of CMC, described hereafter as H-CMC, M-CMC and L-CMC for simplicity, was comparable (ranging from  $0.07 \pm 0.01$  to  $0.1 \pm 0.01$  U/mg). We also tested the activity of FW16.1 against agro-residual biomass (sugarcane bagasse and maize leaves) focusing on the properties of the crude secretome. We therefore prepared lyophilized secretome fractions from both biomass types and resuspended them at a 1:1 ratio. The highest polygalacturonase and laminarinase activity was observed after 24 h, whereas the highest CMCase and xylanase activity was observed after 96 h (Additional file 1: Fig. 4A–D). We observed little activity against arabinan, arabinoxylan, galactan, pectin and starch, either due to low enzymatic specificity for these substrates or the low sensitivity of 3,5-dinitrosalicylic acid (DNS) assay.

### Secretome profiling of *F. metavorans* on synthetic substrates and agro-residual biomass

Tandem mass spectrometric proteomics was used to analyze the FW16.1 secretome fractions, revealing the presence of 500 proteins (Additional file 1: Table S3). Different numbers of proteins were identified on each substrate, ranging from 122 for  $\alpha$ -cellulose to 235 for

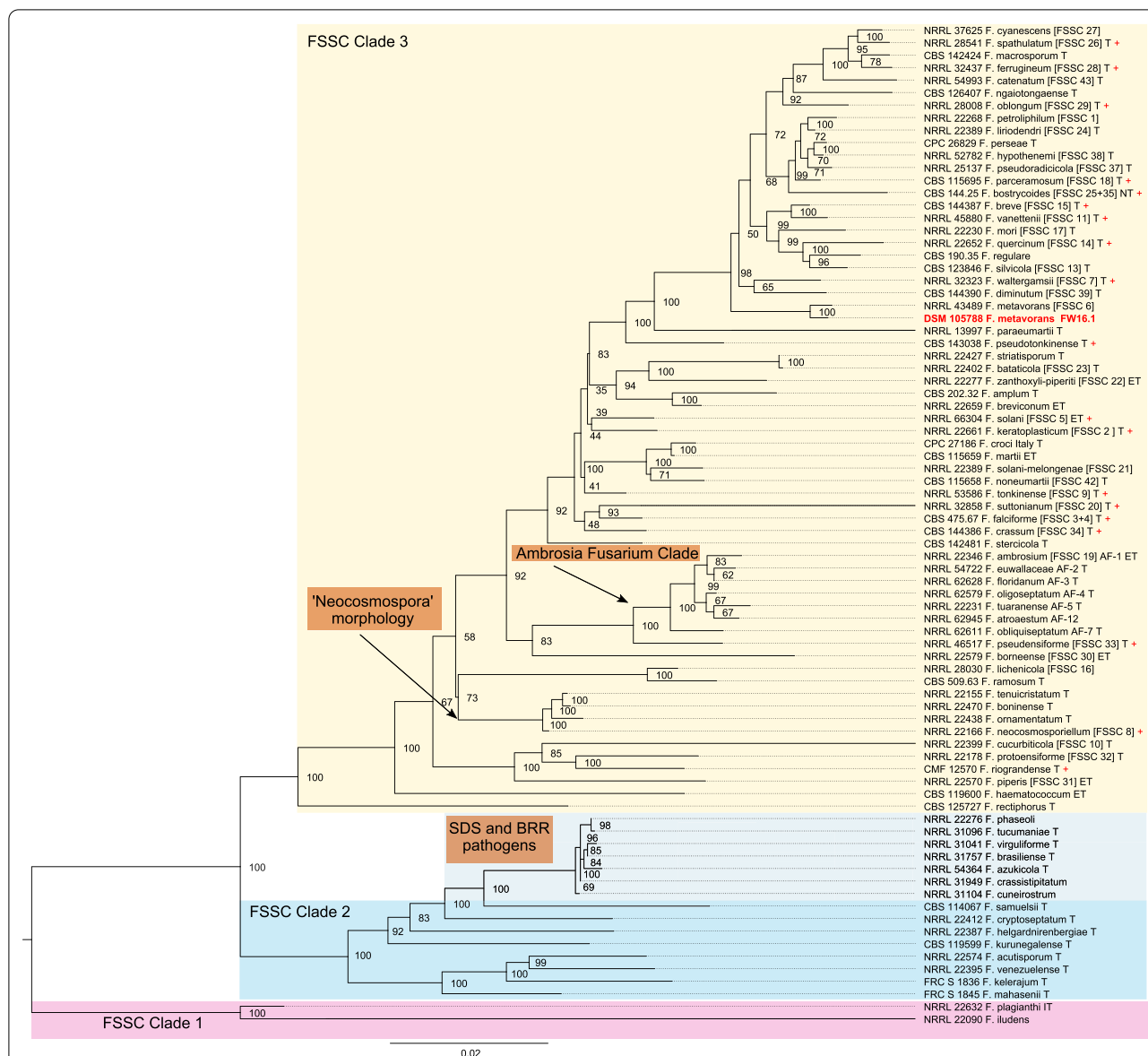
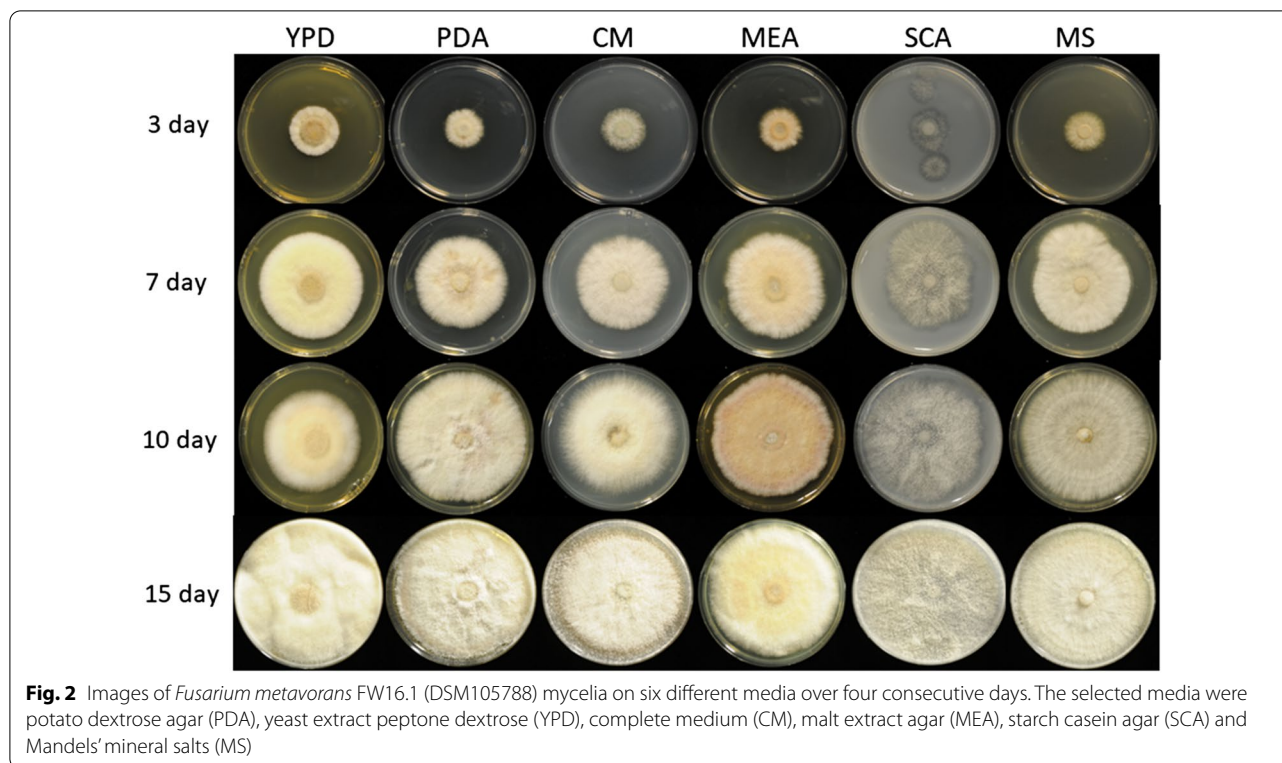


**Fig. 1** Phylogenetic tree of 79 *Fusarium* taxa plus FW16.1 estimated by partitioned maximum likelihood bootstrapping. Numbers at internal nodes indicate branch support based on 5000 data pseudo-replicates in IQ-TREE. The tree was rooted at NRRL 22,090 *F. iludens* and NRRL 22,632 *F. plagianthi*. The alignment holds 3209 columns and 1024 distinct patterns, of which 658 are parsimony-informative, 258 are singletons, and 293 are constant sites. FSSC numbers in brackets represent the ad hoc nomenclature previously used to distinguish species (10.1128/JCM.02371-07). T = ex-type strains; IT = ex-isotype strain; NT = ex-neotype strain

H-CMC. We identified 124 proteins on Avicel PH-101, 144 on M-CMC, 160 on HEC, 174 on sugarcane bagasse, 176 on maize leaves and 202 on L-CMC. We identified 284 proteins on synthetic or artificial cellulose alone, with the number of unique proteins ranging from six on  $\alpha$ -cellulose and Avicel PH-101 to 65 on H-CMC. We identified 13 unique proteins on M-CMC, 26 on HEC, and 31 on L-CMC. We identified 78 proteins solely in the sugarcane bagasse and maize leaf secretome fractions, 23

unique to sugarcane and 31 unique to maize. The largest number of proteins was co-expressed when FW16.1 was grown on the agro-residual biomass, suggesting some of the proteins may be involved in processes not related to energy metabolism (Fig. 4). The second largest number of proteins was co-expressed when FW16.1 was grown on synthetic and artificial cellulose substrates, reflecting the subset of genes required to metabolize these polymers. The third largest number of proteins was common





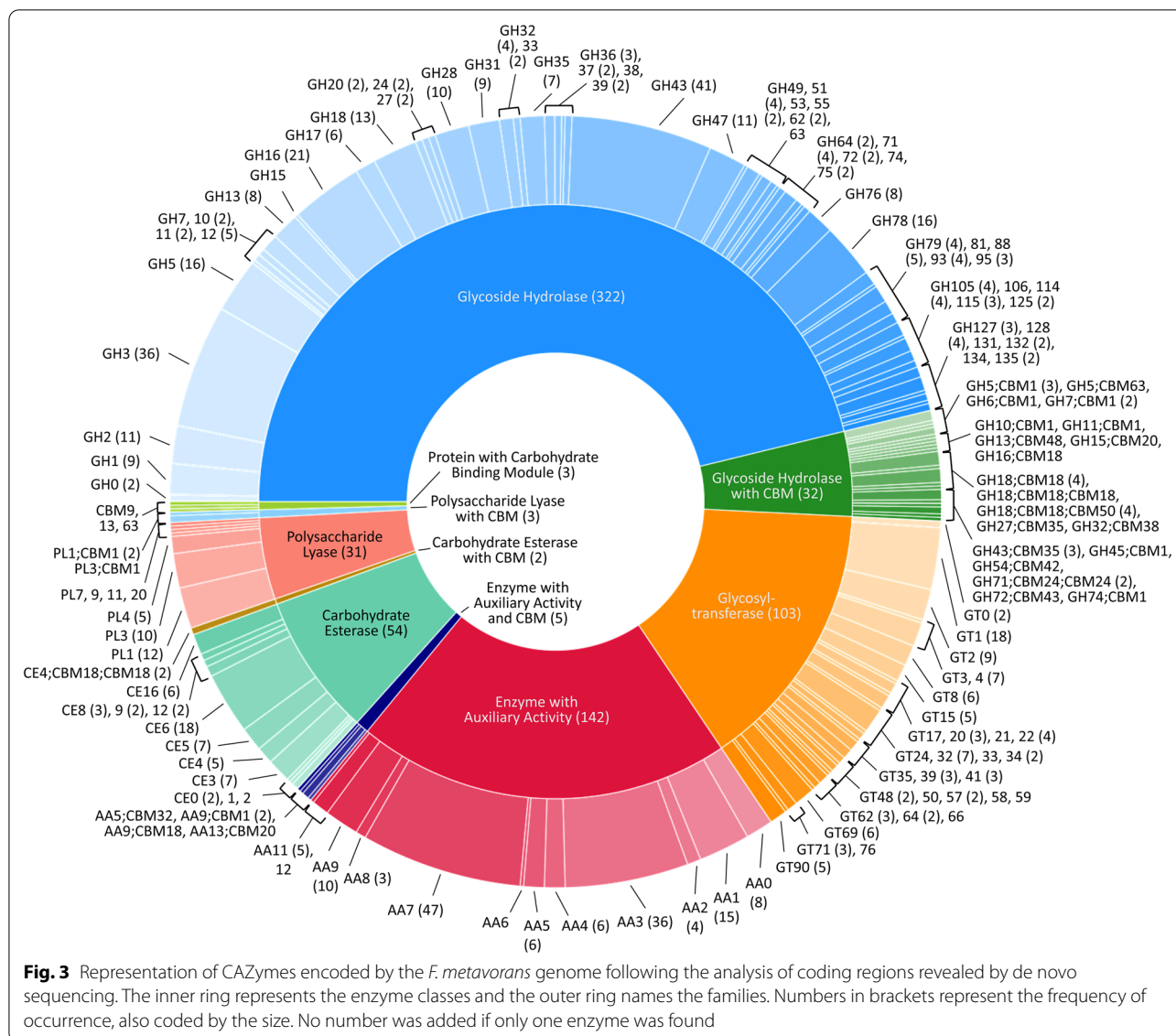
to all conditions, including general sugar conversion and homeostasis genes. Interestingly, the fourth largest group of proteins found on more than one substrate was identified on the CMC media, representing genes specifically required for this artificial substrate. These findings indicate that FW16.1 can fine-tune the expression of relevant genes enabling its survival in different habitats.

The theoretical protein distribution was plotted as a function of isoelectric point (pI) (Fig. 5a) and molecular weight (MW) (Fig. 5b), revealing that 90% of the secretome proteins fell within the MW range 6.5–263.4 kDa (median = 40.8 kDa) and the pI range 2.9–11.8 (median = 5.4). On the six synthetic and artificial cellulose substrates, the median size of the secretome was 38.5–39.5 kDa, but this shifted to 42.5 and 45.1 kDa on the two biomass substrates. Similarly, the median pI was 5.3–5.6 on the synthetic and artificial cellulose substrates, but shifted to 5.0 and 5.1 on maize and sugarcane bagasse, respectively. This effect appears small, but the pI has a logarithmic scale and more than 135 proteins were analyzed for both parameters, resulting in significant deviations ( $p < 0.0001$ ) based on an unpaired  $t$ -test assuming Gaussian distribution (Fig. 5).

To gain insight into the metabolic diversity of the secretome on each substrate, the identified proteins were classified according to biological function (Fig. 5c) based on the sequences listed in Additional file 1: Table S3.

Several molecular functions were identified, including carbohydrate, lipid, RNA and amino acid metabolism, protein synthesis, redox processes, proteolysis, and proteins with unknown functions. The proteins identified on the synthetic and artificial cellulose substrates were distributed similarly according their molecular functions, whereas the relative frequency of proteins related to carbohydrate metabolism was higher on the biomass substrates. The substrate-dependent profiles of the 135 CAZymes are shown in Fig. 5d; a complete list of identified CAZymes with associated modules is provided in Table 2. Predictions based on putative molecular functions for all proteins are summarized in Additional file 1: Table S3. The 135 CAZymes were assigned to five different classes (Table 2): 93 glycoside hydrolases (GHs), 17 auxiliary activities (AAs), 12 carbohydrate esterases (CEs), 12 polysaccharide lyases (PLs), and one glycosyltransferase (GT), as well as three non-catalytic carbohydrate-binding modules (CBMs). The distribution over the scaffolds is presented in Fig. 6.

The most abundant CAZyme class was the GHs (36–58%, or 62–73% when including GHs with CBMs), confirming their general role in cellulose degradation. The lowest proportion of GHs (36%) was identified on the substrate HEC, which also featured the highest proportion of CEs (16%) compared to the median 11%. Another unusual profile was the overrepresentation of PLs on



natural substrates, with 7–8 enzymes (10%) compared to 1–3 (2–6%) on the synthetic and artificial cellulose substrates. The natural substrates also featured more GHs (57–58%), but fewer GH-CBMs (12–14%) than the synthetic and artificial cellulose substrates, which featured 47% GHs and 22% GH-CBMs on average.

Some CAZymes were produced on all substrates, whereas others were more specific. When the “core” GH family proteins (produced on at least five of the six synthetic and artificial celluloses) were evaluated, few differences were found: two GH5, one GH6, two GH7 (all five with CBM1) one GH10, one GH11, one GH16, one GH43, one GH55, one GH71-CBM24-CBM24, one GH72-CBM43, one GH74 and one GH75. Predicted cellulase activities were confirmed in

several cases: endo-β-(1,4)-glucanase activity for FW16\_GLEAN\_10000416 (GH5-CBM1), cellobiohydrolase activity for FW16\_GLEAN\_10006835 (GH6-CBM1), reducing-end cellobiohydrolase activity for FW16\_GLEAN\_10001888 and FW16\_GLEAN\_10005918 (both GH7-CBM1), and potentially xyloglucanase activity for FW16\_GLEAN\_10000631 (GH74). Remarkably, no GH with predicted β-glucosidase activity was found on the cellulose and cellulose-like substrates, whereas FW16\_GLEAN\_10003711 (GH1) and FW16\_GLEAN\_10003498 (GH3) were found on four of the six substrates. Furthermore, enzymes with predicted β-(1,3)-glucanase activity representing GH families 16, 17, 55, 72, 81, 128 and 132 were found mostly on the artificial cellulose substrates and especially on the CMCs,

**Table 1** Identified CAZyme classes based on the *F. metavorans* FW16.1 genome annotation using RAPSearch2 search and HMMER scanning

CAZyme classes	Number of detected genes
Glycoside hydrolases (GH)	322
Glycoside hydrolases (GH) with carbohydrate-binding modules (CBM)	32
Carbohydrate esterases (CE)	54
Carbohydrate esterases (CE) with CBM	2
Polysaccharide lyases (PL)	31
Polysaccharide lyases (PL) with CBM	3
Glycosyl transferases (GT)	103
Glycosyl transferases (GT) with CBM	0
Auxiliary activities (AA)	142
Auxiliary activities (AA) with CBM	5

suggesting the broader substrate specificity of those enzymes or a weak catalytic promiscuity. More diverse cellulose-degrading enzymes were identified on the biomass substrates: FW16\_GLEAN\_10011639 and FW16\_GLEAN\_10004843 (GH3), FW16\_GLEAN\_10001962 (GH5), FW16\_GLEAN\_10006835 (GH6-CBM1) and FW16\_GLEAN\_10005918 (GH7-CBM1), the latter also found on the artificial celluloses.

As suspected, the synthetic and artificial cellulose substrates contained fewer GH family proteins predicted to degrade hemicellulose or pectin compared

to the biomass: FW16\_GLEAN\_10000066 (GH2), FW16\_GLEAN\_10001573 (GH10) and FW16\_GLEAN\_10013304 (GH11), FW16\_GLEAN\_10003286, FW16\_GLEAN\_10006822 and FW16\_GLEAN\_10010955 (GH43). However, a similar distribution was found under both conditions for  $\beta$ -galactosidase (FW16\_GLEAN\_10000066, GH2) a potential xylan  $\beta$ -(1,4)-xylosidase (FW16\_GLEAN\_10011639, GH3),  $\beta$ -(1,3)-glucosidase (FW16\_GLEAN\_10010890, GH17), exo-polygalacturonase (FW16\_GLEAN\_10001538 and FW16\_GLEAN\_10005091, both GH28), and potential disaccharide hydrolases such as FW16\_GLEAN\_10003104 (GH39), FW16\_GLEAN\_10001518, FW16\_GLEAN\_10009840 and FW16\_GLEAN\_10011918 (all GH43) and two exo- $\alpha$ -L-(1,5)-arabinanases (FW16\_GLEAN\_10001805 and FW16\_GLEAN\_10011917, both GH93). GH proteins identified solely on sugarcane bagasse were related to xylan, amylase and dextran degradation (GH10, GH13, and four of the 11 GH43 and GH49 proteins). In contrast, those identified solely on maize leaves were primarily related to disaccharide hydrolysis, including FW16\_GLEAN\_10006734 (GH1), FW16\_GLEAN\_10003498 and FW16\_GLEAN\_10008834 (both GH3,  $\beta$ -glucosidase), FW16\_GLEAN\_10000618 (GH35,  $\beta$ -galactosidase or  $\beta$ -(1,3)-galactosidase) and two of the 11 GH43 proteins (FW16\_GLEAN\_10007175  $\beta$ -D-galactofuranosidase, and FW16\_GLEAN\_10001821, predicted arabinanase or xylosidase).

A clearer picture emerged for the AAs. The synthetic and artificial cellulose substrates mainly featured AA9 proteins with lytic cellulose monooxygenase activity,

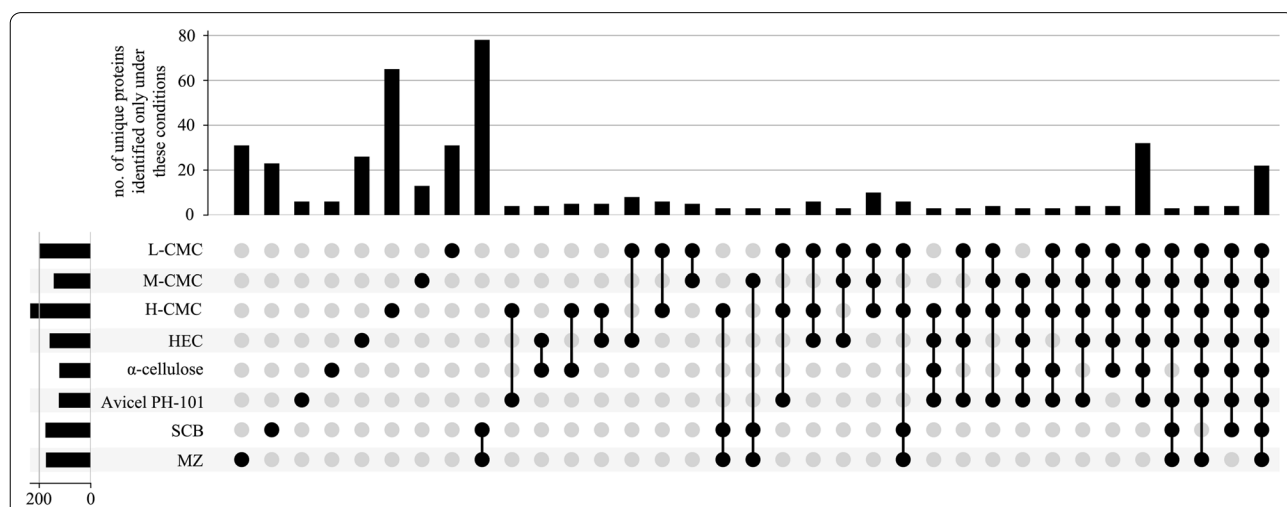
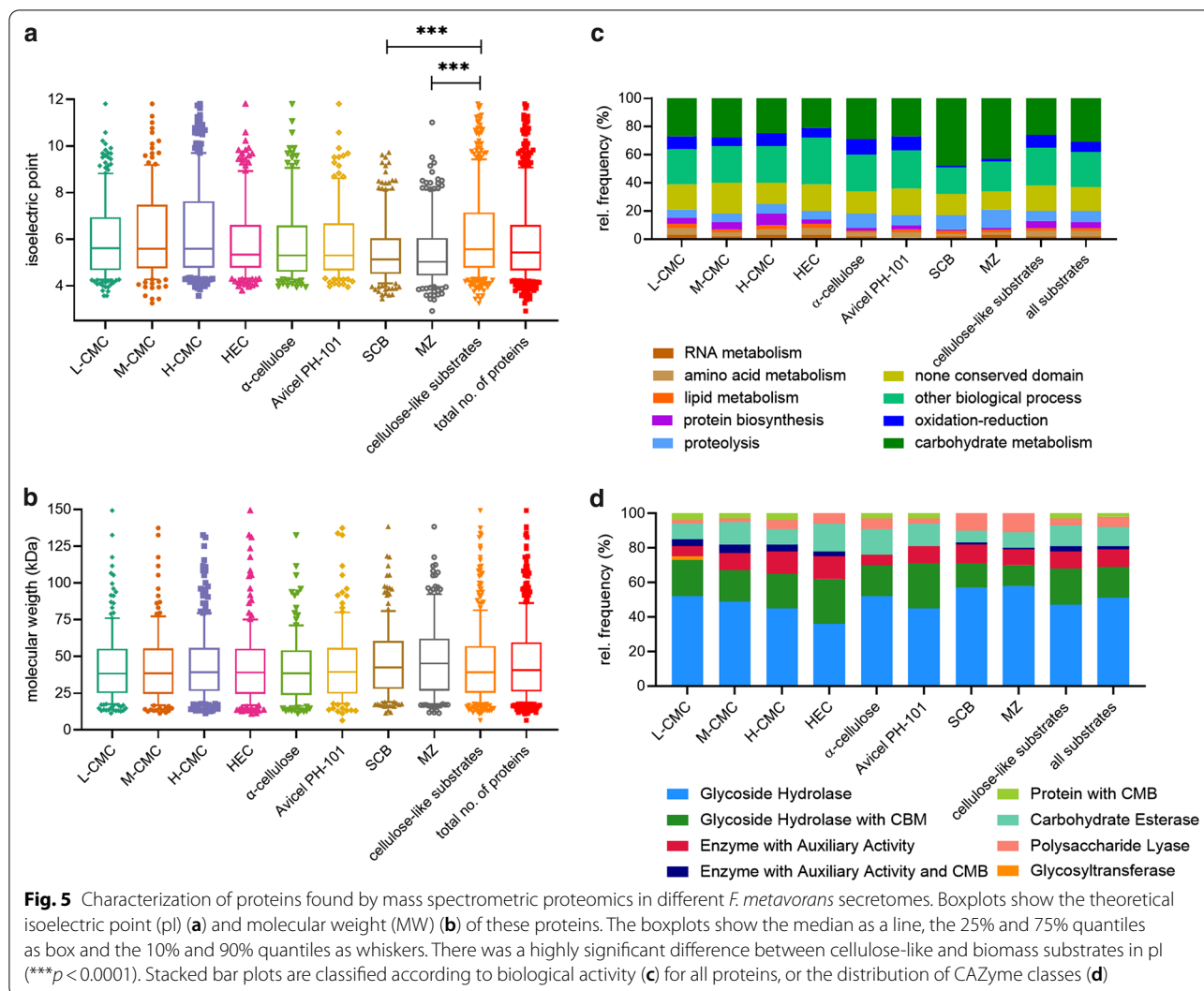


**Fig. 4** Co-expression of proteins found by mass spectrometric proteomics in different *F. metavorans* secretomes. The connected black dots in the lower part of the figure indicate growth conditions resulting in the expression of a shared set of proteins. The number of proteins found under the specific condition is shown by the size of the black bars. The combinations are sorted to first show the unique proteins, which are specific for certain growth media, and the set of proteins found in all conditions last. From all the possible combinations, only those with more than two co-expressed proteins are shown



whereas the biomass substrates showed a greater diversity of AA families. Some were predicted to modify lignin, such as the laccases FW16\_GLEAN\_10001275 and FW16\_GLEAN\_10013360 (both AA1), the alcohol oxidase FW16\_GLEAN\_10000205 (AA3), the cellobiose dehydrogenase FW16\_GLEAN\_10000721 (AA3), and glyoxal oxidase FW16\_GLEAN\_10000164 (AA5). Interestingly, no AA9 proteins were found on maize leaves, but two of the four identified AA9 proteins were found on sugarcane bagasse.

Among the 12 identified PLs, six were found on sugarcane bagasse and 10 were found on maize, highlighting their role in pectin degradation. Only 1–3 PLs were found on the synthetic and artificial cellulose substrates, with FW16\_GLEAN\_10000207 (PL20, predicted endo- $\beta$ -(1,4)-glucuronan lyase) present on five of the six cellulase substrates but not on the biomass substrates.

We identified 4–5 CEs restricted to the synthetic and artificial cellulose substrates, five produced on sugarcane, and seven produced on maize. In the latter case, roles in hemicellulose and pectin degradation are likely, such as FW16\_GLEAN\_10004777 (CE1) and FW16\_GLEAN\_10007169 (CE5), both with predicted (acetyl)xylan esterase activity, FW16\_GLEAN\_10001547 and FW16\_GLEAN\_10001601 (both CE8), FW16\_GLEAN\_10012229 and FW16\_GLEAN\_10013316 (both CE12), all four with predicted pectinase activity. Sugarcane bagasse contained both CE12 enzymes also found on maize leaves, as well as one common CE8 and CE4 protein, and the CE1 protein FW16\_GLEAN\_10014832 with predicted feruloyl esterase activity. CEs solely present on the synthetic and artificial cellulose substrates included FW16\_GLEAN\_10001089 (CE2, acetylxyloxyesterase), FW16\_GLEAN\_10006900 (CE5, pectin esterase), FW16\_GLEAN\_10011996 (CE8, cutinase)





**Table 2** (continued)

No	Accession IDs	Family	Molecular function prediction /Possible substrate(s)	Carbon Source								
41	FW16_GLEAN_10004843	GH3	$\beta$ -Glucosidase								found	found
42	FW16_GLEAN_10001962	GH5	Endo- $\beta$ -(1,4)-glucanase / cellulase / other								found	found
43	FW16_GLEAN_10004691	GH5	Glucan endo- $\beta$ -(1,6)-glucosidase									found
44	FW16_GLEAN_10015175	GH5	Endo- $\beta$ -(1,6)-galactanase									found
45	FW16_GLEAN_10015497	GH5	Mannan endo- $\beta$ -(1,4)-mannosidase	found	found	found						
46	FW16_GLEAN_10007085	GH7	$\beta$ -(1,4)-Glucanase	found	found	found				found	found	found
47	FW16_GLEAN_10003305	GH10	Endo- $\beta$ -(1,4)-xylanase									found
48	FW16_GLEAN_10001573	GH10	Endo- $\beta$ -(1,4)-xylanase	found	found	found	found	found	found	found	found	found
49	FW16_GLEAN_10013304	GH11	Endo- $\beta$ -(1,4)-xylanase	found	found	found	found	found	found	found	found	found
50	FW16_GLEAN_10001797	GH12	Xyloglucan hydrolase				found	found				
51	FW16_GLEAN_10008963	GH12	Xyloglucan hydrolase	found			found	found			found	found
52	FW16_GLEAN_10001440	GH13	$\alpha$ -Amylase								found	
53	FW16_GLEAN_10009774	GH16	Endo- $\beta$ -(1,4)-galactosidase / chitin $\beta$ -(1,6)-glucanosyltransferase / $\beta$ -transglycosidase / $\beta$ -glycosidase / $\beta$ -carrageenase/ endo- $\beta$ -(1,3)-glucanase / laminarinase/ licheninase								found	found
54	FW16_GLEAN_10010201	GH16	Chitin $\beta$ -(1,6)-glucanosyltransferase / $\beta$ -transglycosidase / endo- $\beta$ -(1,3)-glucanase / laminarinase			found		found			found	found
55	FW16_GLEAN_10003917	GH16	Endo- $\beta$ -(1,4)-galactosidase / chitin $\beta$ -(1,6)-glucanosyltransferase / $\beta$ -transglycosidase / $\beta$ -glycosidase / $\beta$ -carrageenase/ endo- $\beta$ -(1,3)-glucanase / laminarinase/ licheninase									found
56	FW16_GLEAN_10009225	GH16	Chitin $\beta$ -1,6)-glucanosyltransferase / $\beta$ -transglycosidase / endo- $\beta$ -(1,3)-glucanase / laminarinase	found	found	found	found	found	found	found		found
57	FW16_GLEAN_10013346	GH16	Endo- $\beta$ -(1,3)-galactanase	found	found	found	found	found				
58	FW16_GLEAN_10004522	GH17	Glucan endo- $\beta$ -(1,3)-glucosidase / licheninase / ABA-specific $\beta$ -glucosidase / $\beta$ -(1,3)-glucanosyltransglycosylase / $\beta$ -(1,3)-glucosidase	found		found				found		
59	FW16_GLEAN_10010890	GH17	$\beta$ -(1,3)-Glucanosyltransglycosylase / $\beta$ -(1,3)-glucosidase								found	found
60	FW16_GLEAN_10012536	GH17	$\beta$ -(1,3)-Glucanosyltransglycosylase / $\beta$ -(1,3)-glucosidase		found						found	found
61	FW16_GLEAN_10013337	GH17	$\beta$ -(1,3)-Glucanosyltransglycosylase / $\beta$ -(1,3)-glucosidase	found		found		found			found	found
62	FW16_GLEAN_10014742	GH17	$\beta$ -(1,3)-glucosidase	found	found	found		found				
63	FW16_GLEAN_10011231	GH18	Chitinase			found					found	found
64	FW16_GLEAN_10006294	GH20	$\beta$ -Hexosaminidase								found	found
65	FW16_GLEAN_10007529	GH24	Lysozyme	found	found	found						
66	FW16_GLEAN_10000319	GH28	Exo-polygalacturonase / xylogalacturonan hydrolase								found	found
67	FW16_GLEAN_10001538	GH28	Exo-polygalacturonase								found	found
68	FW16_GLEAN_10005091	GH28	Exo-polygalacturonase								found	found
69	FW16_GLEAN_10008243	GH28	Exo-polygalacturonase									found
70	FW16_GLEAN_10014771	GH31	$\alpha$ -Glucosidases									found
71	FW16_GLEAN_10011615	GH32	Fructan:fructan 1-fructosyltransferase									found
72	FW16_GLEAN_10000618	GH35	$\beta$ -Galactosidase / $\beta$ -(1,3)-galactosidase									found
73	FW16_GLEAN_10002565	GH37	$\alpha$ , $\alpha$ -Trehalase	found		found					found	found
74	FW16_GLEAN_10003104	GH39	$\beta$ -Glucosidase / $\beta$ -galactosidase/ $\beta$ -xylosidase / $\alpha$ -L-arabinofuranosidase								found	found
75	FW16_GLEAN_10001518	GH43	$\beta$ -Xylosidase / $\alpha$ -L-arabinofuranosidase								found	found

**Table 2** (continued)

No	Accession IDs	Family	Molecular function prediction /Possible substrate(s)	Carbon Source								
76	FW16_GLEAN_10000829	GH43	$\alpha$ -(1,2)-L-Arabinofuranosidase / exo- $\alpha$ -(1,5)-L-arabinofuranosidase / exo- $\alpha$ -(1,5)-L-arabinanase / $\beta$ -(1,3)-xylosidase /exo- $\alpha$ -(1,5)-L-arabinanase / $\beta$ -xylosidase								found	
77	FW16_GLEAN_10003286	GH43	Endo- $\alpha$ -(1,5)-L-arabinanase	found	found						found	
78	FW16_GLEAN_10006822	GH43	$\beta$ -Xylosidase / $\alpha$ -L-arabinofuranosidase	found	found	found	found	found	found	found		
79	FW16_GLEAN_10007175	GH43	$\beta$ -D-Galactofuranosidase									found
80	FW16_GLEAN_10009840	GH43	$\alpha$ -L-Arabinofuranosidase								found	found
81	FW16_GLEAN_10010955	GH43	$\beta$ -Xylosidase	found								
82	FW16_GLEAN_10001821	GH43	$\alpha$ -(1,2)-L-Arabinofuranosidase / exo- $\alpha$ -(1,5)-L-arabinofuranosidase / exo- $\alpha$ -(1,5)-L-arabinanase / $\beta$ -(1,3)-xylosidase /exo- $\alpha$ -(1,5)-L-arabinanase / $\alpha$ -L-arabinofuranosidase									found
83	FW16_GLEAN_10011918	GH43	$\alpha$ -(1,2)-L-Arabinofuranosidase / exo- $\alpha$ -(1,5)-L-arabinofuranosidase / exo- $\alpha$ -(1,5)-L-arabinanase / $\beta$ -(1,3)-xylosidase /exo- $\alpha$ -(1,5)-L-arabinanase / $\alpha$ -L-arabinofuranosidase								found	found
84	FW16_GLEAN_10012038	GH43	$\beta$ -Xylosidase / $\alpha$ -L-arabinofuranosidase								found	
85	FW16_GLEAN_10012117	GH49	Dextranase	found							found	
86	FW16_GLEAN_10003329	GH51	$\alpha$ -L-Arabinofuranosidase								found	found
87	FW16_GLEAN_10014327	GH53	Endo- $\beta$ -(1,4)-galactanase			found						
88	FW16_GLEAN_10002430	GH54	$\alpha$ -L-Arabinofuranosidase								found	found
89	FW16_GLEAN_10003512	GH55	Exo- $\beta$ -(1,3)-glucanase	found	found	found		found	found			
90	FW16_GLEAN_10008698	GH71	$\alpha$ -(1,3)-Glucanase			found						
91	FW16_GLEAN_10004186	GH72	$\beta$ -(1,3)-Glucanosyltransferase								found	found
92	FW16_GLEAN_10013550	GH72	$\beta$ -(1,3)-Glucanosyltransferase	found	found	found	found	found	found	found	found	found
93	FW16_GLEAN_10000631	GH74	Xyloglucanase	found	found	found	found	found	found	found	found	found
94	FW16_GLEAN_10007311	GH75	Chitosanase	found	found	found	found	found	found	found		
95	FW16_GLEAN_10004573	GH79	$\beta$ -Glucuronidase / $\beta$ -4-O-methylglucuronidase								found	found
96	FW16_GLEAN_10011474	GH81	Endo- $\beta$ -(1,3)-glucanase	found	found	found			found			
97	FW16_GLEAN_10001805	GH93	Exo- $\alpha$ -L-(1,5)-arabinanase								found	found
98	FW16_GLEAN_10011917	GH93	Exo- $\alpha$ -L-(1,5)-arabinanase								found	found
99	FW16_GLEAN_10012182	GH99	Glycoprotein endo- $\alpha$ -(1,2)-mannosidase			found	found	found	found	found	found	
100	FW16_GLEAN_10003277	GH115	Xylan $\alpha$ -(1,2)-glucuronidase								found	found
101	FW16_GLEAN_10001958	GH115	Xylan $\alpha$ -(1,2)-glucuronidase									found
102	FW16_GLEAN_10005637	GH128	$\beta$ -(1,3)-Glucanase / $\beta$ -(1,3)-glucosidase	found						found		
103	FW16_GLEAN_10006366	GH132	Glycosidases, potential activity on $\beta$ -(1,3)-glucan	found	found			found				
104	FW16_GLEAN_10010582	GH134	Endo- $\beta$ -(1,4)-mannanase	found	found	found		found				
105	FW16_GLEAN_10000830	GH146	$\beta$ -L-Arabinofuranosidase								found	found
106	FW16_GLEAN_10000416	GH5-CBM1	Endo- $\beta$ -(1,4)-glucanase / cellulase	found	found	found	found	found	found	found		
107	FW16_GLEAN_10004889	GH5-CBM1	Mannan endo- $\beta$ -(1,4)-mannosidase	found	found	found	found	found	found	found	found	found
108	FW16_GLEAN_10006835	GH6-CBM1	Cellobiohydrolase	found	found	found	found		found	found	found	found
109	FW16_GLEAN_10001888	GH7-CBM1	Reducing end-acting cellobiohydrolases	found	found	found	found	found	found	found		
110	FW16_GLEAN_10005918	GH7-CBM1	Reducing end-acting cellobiohydrolase/ chitosanase	found	found	found	found	found	found	found	found	found
111	FW16_GLEAN_10010356	GH11-CBM1	Endo- $\beta$ -(1,4)-xylanase								found	found
112	FW16_GLEAN_10002866	GH13-CBM48	$\alpha$ -(1,4)-Glucan branching enzyme				found					
113	FW16_GLEAN_10004332	GH15-CBM20	Glucosyltransferase	found		found		found				
114	FW16_GLEAN_10007569	GH16-CBM18	Chitin $\beta$ -(1,6)-glucanosyltransferase / $\beta$ -transglycosidase / $\beta$ -glycosidase / $\beta$ -carrageenase /endo- $\beta$ -(1,3)-glucanase / laminarinase			found						
115	FW16_GLEAN_10008961	GH18-CBM18	Chitinase	found								
116	FW16_GLEAN_10002083	GH18-CBM18-CBM50	Chitinase	found								
117	FW16_GLEAN_10008188	GH18-CBM18-CBM50-CBM50	Chitinase								found	found

**Table 2** (continued)

No	Accession IDs	Family	Molecular function prediction /Possible substrate(s)	Carbon Source										
118	FW16_GLEAN_10001593	GH27-CBM35	$\alpha$ -galactosidase / $\beta$ -L-arabinopyranosidase										found	found
119	FW16_GLEAN_10000952	GH43-CBM35	$\beta$ -Xylosidase (subfamily 24)										found	
120	FW16_GLEAN_10007861	GH45-CBM1	Endoglucanase	found			found						found	found
121	FW16_GLEAN_10014717	GH71-CBM24-CBM24	$\alpha$ -(1,3)-Glucanase	found	found	found	found	found	found	found	found		found	found
122	FW16_GLEAN_10012817	GH72-CBM43	$\beta$ -(1,3)-Glucanosyltransglycosylase	found	found	found	found	found	found	found	found		found	found
123	FW16_GLEAN_10004549	GT20	Trehalose 6-phosphatase	found										
124	FW16_GLEAN_10001028	PL1	Pectate lyase										found	found
125	FW16_GLEAN_10001932	PL1	Pectate lyase										found	found
126	FW16_GLEAN_10012037	PL1	Pectate lyase										found	found
127	FW16_GLEAN_10000141	PL3	Pectate lyase				found			found	found			found
128	FW16_GLEAN_10001949	PL3	Pectate lyase										found	found
129	FW16_GLEAN_10008463	PL3	Pectate lyase										found	found
130	FW16_GLEAN_10012035	PL3	Pectate lyase				found	found						
131	FW16_GLEAN_10008683	PL4	Rhamnogalacturonan lyase											found
132	FW16_GLEAN_10015384	PL4	Rhamnogalacturonan lyase											found
133	FW16_GLEAN_10001628	PL9	Pectate lyase / exopolysaccharonate lyase / rhamnogalacturonan endolyase										found	found
134	FW16_GLEAN_10000207	PL20	Endo- $\beta$ -(1,4)-glucuronan lyase	found	found	found	found	found	found	found				
135	FW16_GLEAN_10013878	PL3-CBM1	Pectate lyase											found

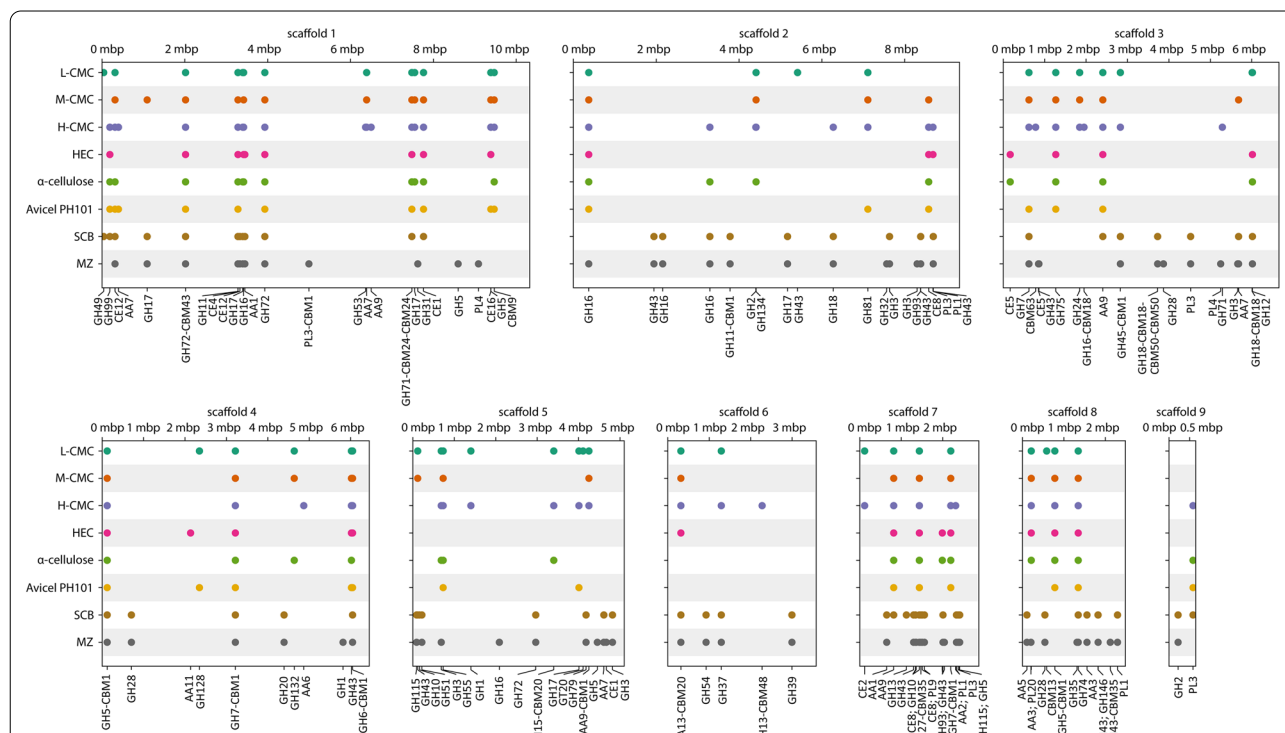


**Fig. 6** Mapping of 135 CAZymes found by mass spectrometric proteomics in different *F. metavorans* secretomes. *F. metavorans* FW16.1 was grown on eight different substrates (y-axis) differing in complexity. The CAZymes identified by MS were mapped back to protein coding regions (CDS) in our de novo genome assembly, which consists of nine scaffolds. A circle indicates the genomic location of a CDS with a positive proteomics mapping. The circle color corresponds to the growth substrate. The CDS is annotated with its CAZyme family name on the x-axis. For example, the same CDS on scaffold 2, annotated as GH16, is expressed/secreted in all growth substrates except sugarcane bagasse, and is located at position 389,635–390,517 bp (exact position not shown for clarity)

and FW16\_GLEAN\_10015496 (CE16, acetyl esterase). We identified only one GT protein (FW16\_GLEAN\_10004549, GT20) and this was found on the L-CMC substrate.

Finally, we identified proteins representing three CMB families present solely on the synthetic and artificial cellulose substrates: FW16\_GLEAN\_10015530 (CBM9), FW16\_GLEAN\_10000334 (CBM13) and FW16\_GLEAN\_10007143 (CBM63). Interestingly, CBM9 and CBM63 are predicted to bind cellulose but CBM13 is not. Another eight CBM families were represented in the modular proteins described above, combined with GH, AA or PL domains, and these were distributed similarly between the synthetic cellulose and biomass substrates. CBM1 was the most abundant module (nine identified in total), and was associated with GH, AA and PL proteins, whereas the other CBMs were found only 1–3 times each.

#### Conversion of biomass with the in-house *F. metavorans* cocktail

The overall enzymatic activity of the crude secretome preparations was low. We therefore lyophilized the enzymes secreted on both biomass substrates, resuspended them in 50 mM citrate buffer (pH 4.8), and combined them at a 1:1 ratio with a final protein concentration of  $312 \pm 2.7$   $\mu\text{g/mL}$ . We then prepared saturation curves (Additional file 1: Table S5).

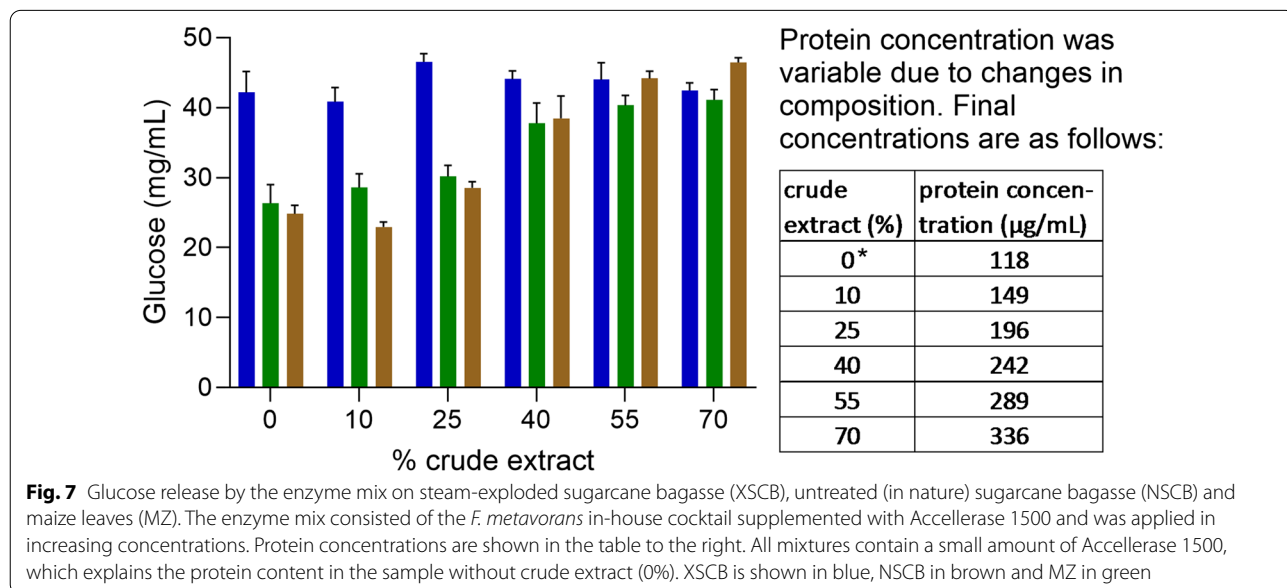
Hydrolysis assays were evaluated against three different substrates: steam-exploded sugarcane bagasse (XSCB), untreated (in nature) sugarcane bagasse (NSCB) and untreated maize leaves (MZ), each present at a concentration of 5% (w/v) for 24 h. Control assays without

in-house enzymes (A1) were also prepared. All assays were supplemented with the commercial Accellerase 1500 enzyme mixture containing exoglucanase, endoglucanase, hemi-cellulase and  $\beta$ -glucosidase at a concentration of 5 FPU/mL (filter paper unit). Under control conditions (A1), XSCB was converted to glucose 1.6-fold more efficiently than the other substrates (Fig. 7). To test the activity of the secretome preparation, we supplemented the assay with the *F. metavorans* in-house cocktail at concentrations ranging from 10% (v/v) in assay A2 to 70% (v/v) in assay A6 (Additional file 1: Table S5).

Figure 7 shows the glucose profile following biomass hydrolysis in all assays (A1–A6). XSCB was easily converted to glucose by the commercial Accellerase 1500 enzyme mix, but the in-house cocktail did not facilitate further saccharification. In contrast, the in-house cocktail enhanced the release of sugars from the NSCB and MZ substrates starting at concentrations of 25% (v/v), corresponding to 196  $\mu\text{g/mL}$ . When the concentration of the in-house cocktail reached 55% (v/v), corresponding to 0.289  $\mu\text{g/mL}$ , the efficiency of saccharification became equivalent to that of the pre-treated (XSCB) substrate. An in-house enzyme cocktail with a protein load of 35–36 mg/g biomass therefore facilitated synergistic depolymerization without pre-treatment, achieving a statistically significant improvement in glucose yields ( $p < 0.05$ , 95% confidence).

#### Discussion

We set out to characterize an active fungal isolate by identifying enzymes that facilitate the utilization of plant biomass, particularly those involved in cellulose





degradation. We compared the enzymes induced by different synthetic cellulose substrates, and analyzed secretome components on two different types of agro-residual biomass representing the C4 crops sugarcane and maize [25, 44]. We also assigned the fungal isolate to the correct FSSC linkage. To the best of our knowledge, this is the first comparative analysis of the *F. metavorans* as a strain of the FSSC secretome on different substrates.

Analysis of the 62 proteins produced on all six artificial cellulose substrates revealed only 16 CAZymes, five of which were predicted to degrade cellulose. The enzymes were assigned to CAZy families GH5, GH7 and AA9. The corresponding genes were distributed over four different scaffolds, but there was no clear evidence for clusters of colocalized or coregulated genes. The hydrolytic degradation of cellulose by fungi involves at least three steps: (1) internal cellulose bonds are cleaved by endo- $\beta$ -(1,4)-glucanases (GH5) [45–47] to create shorter polymers; (2) these are digested by exo- $\beta$ -(1,4)-glucanases and/or cellobiohydrolases (GH7 and GH6) ultimately to produce cellobiose, which is (3) finally converted into two glucose molecules by  $\beta$ -glucosidases (mainly GH1 or GH3, and some others such as GH39) [48, 49]. At least the first two steps were recapitulated in the *F. metavorans* FW16.1 secretome fractions. For the first step, one predicted GH5 protein with cellulase activity (FW16\_GLEAN\_10000416) was found on all cellulose substrates, whereas another (FW16\_GLEAN\_10001962) was found on the biomass substrates. For the second step, one GH7 with a CBM1 domain (FW16\_GLEAN\_10005918, predicted cellobiohydrolase) was found on all substrates, another (FW16\_GLEAN\_10001888) was found on the artificial cellulose substrates, and a third without a CBM (FW16\_GLEAN\_10007085) was found on six of the eight substrates. Some proteins with predicted  $\beta$ -glucosidase activity (GH1, GH3 maybe GH39) were also found, but none of them were present on all substrates.

We also identified an AA9 lytic polysaccharide monooxygenase (LPMO) that can oxidize the C-1 or C-4 (and perhaps C-6) positions of the glycosidic bond in cellulose and disrupt its structure, as shown for the fungi *Podospora anserina* and *Neurospora crassa* [50, 51]. An interesting combination of AA9 and PL20 was observed, where glycosidic bonds of glucuronic acid-containing cello-oligosaccharides produced by AA9 proteins may be cleaved at the C4-position by the PL20 family via  $\beta$ -elimination to produce a reducing end [52]. This mechanism could also be involved in cellulose degradation, as already postulated for the fungus *Humicola insolens* [53]. A clear difference in cellulose degradation was identified between the biomass substrates, with more GHs found on maize leaves contrasting with more AAs catalyzing oxidative cellulose degradation on sugarcane

bagasse, the latter indicating a more complex cellulose architecture [54]. The GH74 family, with predicted xyloglucanase activity, was also found on all substrates, and may therefore contribute to cellulose degradation. This is supported by the identification of a GH74 xyloglucanase from the bacterium *Cellvibrio japonicas* with a strong preference for xyloglucans but some activity (24–165-fold lower) against artificial substrates such as CMC and HEC [55]. Another protein (AA13) fused to the starch-binding module CBM20 [56] was found on four of the six synthetic cellulose substrates, perhaps indicating promiscuous activity against artificial celluloses. However, no cellulase activity was previously reported for AA13 enzymes isolated from the fungi *Neurospora crassa* and *Aspergillus nidulans* [57, 58].

The distribution of the CAZymes on the two biomass substrates was more complex, mirroring the complexity the substrates, including the presence of hemicellulose, pectin and lignin. The secretome fractions thus included a lignocellulolytic enzyme cocktail with the ability to degrade all cell wall polymers and stored starch granules, including cleavage by lyases and oxidation.

The degradation of hemicellulose requires enzymes specific for  $\beta$ -(1,4)-linked xyloses or xyloglucan and arabinoxylan acetylated at the C2 and/or C3 positions as well as  $\beta$ -(1,3),  $\beta$ -(1,4) and  $\beta$ -(1,6) glucan branches [59] that connect pectin to cellulose [17, 60]. These include endo- $\beta$ -(1,4)-xylanases (GH10, GH11),  $\alpha$ -L-arabinofuranosidases and exo- $\alpha$ -L-(1,5)-arabinanases (GH3, GH43, GH51, GH54, GH62 and GH93),  $\beta$ -xylosidases (GH43 and GH3), acetylxylan esterases (CE1–CE7), and ferulic acid esterases (CE1) and acetyl esterases (CE16) [48]. We found three GH10 and GH11 proteins on maize and four on sugarcane. We also found GH27-CBM35, GH31 and GH35 proteins (the latter two restricted to maize) two GH93 proteins and one GH115 protein, all probably responsible for hemicellulose or rhamnogalacturonan I (pectin) degradation [61]. The GH43 family, which converts xylo-oligosaccharides containing arabinose and galactose to monomers, was also found on both substrates. We identified 11 GH43 enzymes in total, three exclusively on sugarcane and two on maize. Previous secretome analysis of *Trichoderma reesei* and *Aspergillus niger* on sugarcane bagasse [62], *A. nidulans* on sorghum [60], *Myceliophthora thermophila* on sugarcane bagasse [63] and *N. haematococca* on maize bran [64] identified one, five, eight, four and four GH43 proteins, respectively. We also identified multiple xylan esterases (CE1, CE4 and CE5): three on maize and one on sugarcane, similar to the *T. reesei* secretome on sugarcane bagasse which features two CE5 proteins [62]. In contrast, no CEs were found in the secretome fractions of *N. haematococca* on maize bran [64].

A combination of GHs, CEs and PLs was needed to break down pectin in our biomass substrates [19]. The GHs we identified represented families GH28 (four in total, one only found on sugarcane), GH43 and GH79 [19], perhaps also including GH35, GH51 and GH93 (which can digest rhamnogalacturonan I) [65]. We identified three CE8 proteins (two found only on sugarcane) and two CE12 proteins (required to remove branches from non-sugar components containing methyl and acetyl groups). Finally, we identified six PLs from families PL1, PL3 and PL9 on sugarcane, and 10 PLs from families PL1, PL3, PL4 and PL9 on maize. These are necessary for the efficient utilization of homogalacturonan and rhamnogalacturonan. In contrast, no pectin-digesting GHs, CEs and PLs were identified in the secretome of *N. haematococca* on maize bran, whereas the *A. niger* BRFM442 secretome contained six GH28, two CE8 and one PL proteins on the same substrate [64].

The AA superfamily of lignolytic enzymes and monooxygenases [66] was also found in the secretome induced on our maize and sugarcane substrates. Laccases (AA1) oxidize a wide range of aromatic compounds including polyphenols, methoxy-substituted monophenols and aromatic amines [67] and these were found on both substrates. When other *F. solani* strains were cultured on substrates such as oak combined with millet and wheat bran or corn, wheat, rye and oat, the secretome fractions contained laccases as well as manganese-dependent peroxidases (MnP) and lignin peroxidases (LiP), both of which represent family AA2 [68, 69]. We did not find any AA2 proteins, perhaps because we investigated only a limited set of time points, thus providing an incomplete picture of oxidative lignin degradation. However, we identified AA3 flavoenzymes on both substrates, and this family includes glucose oxidases and aryl alcohol oxidases that act on the anomeric carbon of  $\beta$ -D-glucose and alcohols using molecular oxygen as an electron acceptor, releasing hydrogen peroxide [70]. It is interesting to note that feruloyl and *p*-coumaroyl esterases were not found on the maize substrate, whereas one CE1 protein with that predicted function was found on sugarcane and all the cellulose substrates. These esterases normally remove the crosslinks between polysaccharides and lignin to increase enzymatic access to the cell wall [62, 63]. The analysis of an *A. nidulans* strain on sorghum stover revealed only two esterases in the secretome [54].

Several of the enzymes discussed above overcome the inaccessibility of insoluble substrates by using one or more non-catalytic CBMs [71]. Examples include the GH5, GH7, GH11, GH45 and PL3 families, which are frequently associated with CBM1 (which typically binds cellulose) [72]. Three of the five GH18 family members we identified were associated with the chitin-binding

modules CBM18 and CBM50. Similarly, the *T. reesei* genome encodes at least 18 GH18 proteins, four with additional CBMs [73]. A glucoamylase (GH15) associated with the starch-binding module CBM20 was found in *Penicillium echinulatum* [74], and we identified  $\alpha$ -(1,4)-glucan branching enzymes (GH13) associated with the glycogen-binding module CBM48, which has been found in several other species [75]. We also identified an  $\alpha$ -(1,3)-glucanase (GH71) associated with the starch-binding module CBM24, and an  $\alpha$ -galactosidase (GH27) associated with CBM35, which was shown to bind  $\beta$ -galactans in *Phanerochaete chrysosporium* [66].

Our comparative approach revealed 500 secretome proteins, including 93 GH proteins representing 40 different families. A similar range was reported *F. solani* ATCC MYA 4552 cultivated on a mixture of oak, millet and wheat, where 398 proteins were identified, including 48 GH proteins representing 28 families [69]. We compared the secretome proteins of our *F. metavorans* FW16.1 isolate on natural substrates with nine other fungal secretome fractions [60, 62, 64, 76–78]. In most cases, our isolate produced a larger number of secreted CAZymes, with only *A. nidulans* strain A78 grown on sorghum stover and *A. niger* BRFM442 grown on maize bran producing more (Table 3). The cultivation of *N. haematococca* on maize bran produced four GH43 proteins but no members of the families GH5, GH6, GH7 or AA9, arguing that maize bran induces the secretion of hemicellulases [64]. We found that *Fusarium* sp. of the FSSC uses their diverse arsenal of depolymerizing and accessory enzymes as destruenters to break down complex substrates, supported by their adaptation to different environments, their metabolic plasticity, and their ability to degrade different lignocellulose materials [69, 79], as well as other compounds such as the pesticide dichlorodiphenyltrichloroethane [80].

The *F. metavorans* in-house enzymatic cocktail proved a suitable alternative to the chemical pre-treatment of agro-residual lignocellulosic biomass, clearly allowing the debranching of polymers surrounding the cellulose fibers and releasing reducing sugars (Fig. 7). Pre-treatment methods are often needed for recalcitrant biomass such as hemicellulose, lignin and crystalline cellulose, to open up the fibers and improve accessibility to the polymers [44, 81]. Accordingly, the *F. metavorans* in-house cocktail did not enhance the production of sugars from sugarcane biomass subjected to steam explosion, because pre-treatment had already rendered the polymers fully accessible to the Accellerase 15,000 cocktail. However the in-house cocktail had a strong impact on the saccharification of untreated maize and sugarcane biomass, with additional advantages over chemical pre-treatment such as selectivity, mass efficiency (the released carbohydrates

**Table 3** Comparison of CAZymes identified by mass spectrometric proteomics in six different studies encompassing seven different fungi, five different types of biomass, and six different synthetic and artificial cellulose substrates

Strain	Substrates	Fermentation	GHs	CEs	AAs	PLs	GTs	Source
<i>Trichoderma reesei</i> RUT-C30	Exploded sugarcane bagasse	Solid-state	15	0	1	0	0	[62] <sup>a</sup>
<i>T. reesei</i> RUT-C30	Sugarcane culm	Solid-state	19	0	1	0	0	[62] <sup>a</sup>
<i>Aspergillus niger</i> N402	Exploded sugarcane bagasse	Solid-state	35	10	2	1	0	[62] <sup>a</sup>
<i>A. niger</i> N402	Sugarcane culm	Solid-state	34	5	1	1	0	[62] <sup>a</sup>
<i>Fusarium metavorans</i>	In nature sugarcane bagasse	Liquid fermentation	49	8	9	7	0	This work
<i>F. metavorans</i>	Maize leaves	Liquid fermentation	58	11	8	8	0	This work
<i>F. metavorans</i>	L-CMC	Liquid fermentation	39	6	5	1	1	This work
<i>F. metavorans</i>	M-CMC	Liquid fermentation	26	5	6	1	0	This work
<i>F. metavorans</i>	H-CMC	Liquid fermentation	40	7	9	3	0	This work
<i>F. metavorans</i>	HEC	Liquid fermentation	19	6	5	2	0	This work
<i>F. metavorans</i>	α-Cellulose	Liquid fermentation	27	6	2	2	0	This work
<i>F. metavorans</i>	Avicel PH-101	Liquid fermentation	21	4	3	1	0	This work
<i>Nectria haematococca</i>	Maize bran	Liquid fermentation	30	0	3	2	0	[64]
<i>A. niger</i> BRFM 442	Maize bran	Liquid fermentation	77	5	3	1	0	[64]
<i>Trichoderma asperellum</i> S4F8	In nature sugarcane bagasse	Solid-state	61	3	0	0	1	[77]
<i>T. reesei</i> RUT-C30	In nature sugarcane bagasse	Solid-state	37	3	2	0	1	[77]
<i>Trichoderma harzianum</i> P49P11	Exploded sugarcane bagasse	Liquid fermentation	19	0	1	0	0	[78]
<i>T. harzianum</i> IOC 3845	In nature sugarcane bagasse	Liquid fermentation	57	3	1	0	0	[76]
<i>Aspergillus nidulans</i> A78	Sorghum stover	Solid-state	79	5	4	8	0	[60] <sup>a</sup>

<sup>a</sup> Time course analysis

are retained and utilized), and the avoidance of inhibitory by-products. Furthermore, no toxic compounds are dispersed into the environment, avoiding the need to recycle or remove them. The *F. metavorans* enzyme cocktail therefore provides a sustainable, low-energy process to enhance the efficiency of enzymatic saccharification [82–84].

## Conclusion

The CAZymes identified in this study can be used to enhance the enzymatic saccharification of agro-residual biomass. Our workflow involved strain isolation, genome sequencing, CAZyme analysis and secretome analysis by mass spectrometric proteomics, revealing 135 relevant enzymes. The *F. metavorans* in-house cocktail was used to increase the amount of glucose generated from maize leaves and untreated sugarcane bagasse by selective pre-treatment, improving the turnover of the hemicellulose fraction without carbohydrate loss or the formation of inhibitory by-products.

## Materials and methods

### Fungus isolation and growth conditions

The fungal isolate *F. metavorans* FW16.1, was obtained from mangrove wood [43] in Vietnam (longitude 10°36′015″N, latitude 106°56′045″E) and prepared as a conidial suspension. Mycelium pieces (5 mm diameter)

on potato dextrose agar (PDA) were transferred to a fresh PDA plate and grown in the dark for 5–7 days at 28 °C. The conidia were scraped with a Drigalski cell spreader in sterile water and centrifuged at 2693 × *g* for 15 min at 4 °C. The pellet was washed in sterile water, filtered through a 40-μm mesh sieve and centrifuged as above. The pellet was resuspended in sterile water, aliquoted and stored at – 70 °C. To investigate mycelial growth and color formation, fungal growth was assessed on PDA, YPD [85], complete medium (CM) [86], malt extract agar (MEA) [87], starch casein agar (SCA) [88] and Mandel's salt medium (MS) [89] for 15 days (Fig. 2).

### Phylogenetic analysis and de novo sequencing

Submerged cultures of *F. metavorans* FW16.1 were established in potato dextrose broth (PDB) and incubated at 28 °C, shaking at 150 rpm. DNA was isolated according to the CTAB method [90, 91] and purity and quality were confirmed by gel electrophoresis and spectrophotometry. We used 11 μg of pure high-molecular-weight genomic DNA (gDNA) for the de novo preparation of 270-bp short HiSeq and PACBIO RSII 20 K sequencing libraries. Following gene prediction, ORFs were identified and annotated according to Gene Ontology (GO), Kyoto Encyclopedia of Genes and Genomes (KEGG) and Clusters of Orthologous Groups (COGs) using BGI (Beijing Genomics Institute, China) to create a

fungus-specific database (Additional file 2: FW16.IntegrationTable.xls). The genome sequence of *F. metavorans* FW16.1 was deposited in GenBank (bioproject number PRJNA413482, biosample number SAMN07749916) with the accession number JADNRB000000000.

The ITS-1/8S rRNA/ITS-2 region was amplified and sequenced using primers ITS1\_fw (5'-TCC GTA GGT GAA CCT GCG G-3') and ITS4\_rv (5'-TCC TCC GCT TAT TGA TAT GC-3') [92] and the ITS sequence was deposited in GenBank (accession number MG098676). Multiple sequence alignments for marker genes *TEF1*, *RPB2* and ITS + 28S for 79 *Fusarium* taxa were kindly provided by Kerry O'Donnell (personal communication). We built three independent covariance models using cmbuild v1.1.3 in the Infernal package (<https://doi.org/10.1093/bioinformatics/btt509>) from the sequence alignments without consensus structure information (parameter -noss). The bit scores depend on multiple sequence alignment length (more precisely, the covariance model length), so we ran the ungapped alignment sequences against their covariance model (calign -noss -g) and obtained 639, 1668 and 981 bits as average scores for *TEF1*, *RPB2* and ITS + 28S, respectively. Given that a covariance model without a consensus structure is basically a hidden Markov model (HMM), we initially used hmmbuild and hmmsearch ([www.hmm.org](http://www.hmm.org)) instead, but this did not yield hits with sufficient scores, most likely due to high penalties for the insertion of introns.

Using the covariance model for *TEF1*, we found a hit in scaffold2 at position 6,427,210–6,427,837 with 643 bits (slightly above average). The model for *RPB2* returned two partial hits in close proximity on the reverse strand of scaffold 3. Manual inspection revealed overlapping full models for those hits, but a 130-bp region (probably an intron) divided the region in half. Enforcing global alignment of the combined region 2,964,591–2,966,345 (calign -noss -g) resulted in a score of 1671 bits, which was above the expected average score.

The covariance model for the ITS + 28S region did not return significant hits, probably due to the omission of this region in the assembly, reflecting multiple gene copies and repetitive regions that complicated the coverage information [93]. We therefore used the covariance model to identify 5737 of the raw 465,771 PacBio reads with sufficient hits. We next used proovread v2.14.1 (<https://doi.org/10.1093/bioinformatics/btu392>) to polish the frequent insertion or deletion of bases (indels) in the PacBio reads with short Illumina reads and mapped the results against the FW16.1 scaffold using bowtie2 v2.3.4.1 (<https://doi.org/10.1038/nmeth.1923>) with the settings -p 20-very-sensitive-local-f, yielding a clear pile up on scaffold 1 from 2,806,169 to 2,812,396. The local

alignment of 2245 polished reads against the model (calign -mxsize 100,000 -noss) resulted in 456 high-scoring identical alignment rows of 1227 bp. Finally, we added the three identified marker gene regions to the initial sequence alignment (Additional file 3: 79-FSSC-3-locus.nex) and used IQTree v1.6.12 (<https://doi.org/10.1093/molbev/msaa015>) with the settings -nt AUTO -bb 5000, and partitions *TEF1* = 1–665, ITS + 28S = 666–1621 and *RPB2* = 162–3209 to construct the phylogenetic tree with partitioned maximum likelihood bootstrapping. The resulting newick tree file (Additional file 4, tree\_fw16+79.figtree) was rooted at NRRL 22,090 *F. illudens* and NRRL 22,632 *F. plagianthi* and colored using FigTree v1.4.4 (<http://tree.bio.ed.ac.uk/software/figtree/>).

### CAZyme analysis

All genomic regions marked as CDS in our de novo assembly were screened for homologs to families and subfamilies in the CAZyme database [66] using a combination of RAPSearch2 [94, 95] and hmmsearch from the HMMER package [96] as previously described [97]. The CAZyme families/subfamilies were represented by sequence members with different enzymatic activities, annotated as different EC numbers, thus a single homolog CDS can yield multiple EC annotations. To reduce EC number ambiguity, we used BLASTP (v2.9.0+) to score the CDS identified by LC-MS/MS against all sequences of the homologous CAZyme family obtained from dbCAN2 (<http://csbl.bmb.uga.edu/dbCAN/index.php>) [98]. The CDS was only annotated with EC numbers of the top BLASTP hits for each protein. The corresponding descriptors of EC numbers were used as possible functions (Additional file 1: Table S4). CAZymes identified by LC-MS/MS were mapped to the genome.

### Secretome analysis and SDS-PAGE

The *F. metavorans* secretomes were induced by fermentation in 100-mL Erlenmeyer flasks at 28 °C for up to 96 h, shaking at 150 rpm. Each liquid fermentation was carried out in duplicate (agro-residual biomass) or triplicate (synthetic substrates). Mycelia were pre-cultivated in YPD medium at 28 °C for 3 days, shaking at 150 rpm, then washed briefly and dried between sheets of filter paper (Whatman, Dassel, Germany). We then incubated 0.1 g of the semi-dried mycelia with 50 mL inductive medium at 28 °C for 72 h, shaking at 150 rpm. The inductive medium comprised mineral salts (0.35% NaNO<sub>2</sub>, 0.15% K<sub>2</sub>HPO<sub>4</sub>, 0.05% MgSO<sub>4</sub> × 7H<sub>2</sub>O, 0.05% KCl, 0.001% FeSO<sub>4</sub> × 7H<sub>2</sub>O) supplemented with 1% (w/v) synthetic or artificial cellulose (Avicel, α-cellulose, HEC, H-CMC, M-CMC or L-CMC, all from Sigma-Aldrich, Steinheim, Germany). The agro-residual biomass was prepared at a final concentration of 1% in Mandels and Weber medium



[99], with additional yeast extract and peptone (0.03%). The sugarcane bagasse was milled to 1 mm and the maize leaves to 1.5 mm as untreated substrates. After 96 h, the fungal biomass was removed by centrifugation ( $3250 \times g$  for 30 min) and the supernatant was harvested for secretome analysis, followed by lyophilization and resuspension in 50 mM citrate buffer (pH 4.5). The secretome samples were separated by SDS-PAGE on 12% polyacrylamide gels [100]. The gels were stained with 0.1% Coomassie Brilliant Blue R250 and destained with 45% methanol and 10% acetic acid. The gels were set aside for analysis by mass spectrometric proteomics and remaining samples were retained for enzymatic assays.

## Proteomics

### Sample preparation

In-gel tryptic digestion [101] was carried out by dividing each gel lane into 4–5 equal parts and dicing them, followed by reduction with 10 mM dithiothreitol in 100 mM ammonium bicarbonate, alkylation with 55 mM iodoacetamide in 100 mM ammonium bicarbonate and digestion with 13 ng/ $\mu$ L trypsin in 10 mM ammonium bicarbonate containing 10% (v/v) acetonitrile (Promega, Mannheim, Germany). Tryptic peptides were extracted with a 1:1 mixture of 5% formic acid and acetonitrile and were completely lyophilized. The peptides were resuspended in 40  $\mu$ L 0.1% formic acid before LC–MS/MS analysis.

### LC–MS/MS analysis of the tryptic peptides

We injected 2- $\mu$ L samples onto an Acclaim PepMap C-18 nanoViper trapping column (Thermo Fisher Scientific, Waltham, MA, USA; 100  $\mu$ m  $\times$  20 mm, 5  $\mu$ m, 100 Å) at a flow rate of 3  $\mu$ L/min and washed for 5 min with 2% buffer B (0.1% formic acid in acetonitrile). The peptides were separated on an Acclaim PepMap C-18 nanoViper reversed-phase capillary column (Thermo Fisher Scientific; 75  $\mu$ m  $\times$  50 cm, 2  $\mu$ m, 100 Å) at 45 °C using a Dionex Ultimate 3000 nano-UPLC system (Thermo Fisher Scientific) connected to a Fusion tribrid (quadrupole/Orbitrap/linear ion-trap) mass spectrometer (Thermo Fisher Scientific). The gradient system consisted of buffer A (0.1% formic acid in MS-grade water) and buffer B at a constant flow rate of 300 nL/min for 70 min. The profile was held at 3% B for 5 min followed by a gradient to 28% B, at 35 min, then 35% B at 40 min, and 90% B at 40 min 6 s. After a hold at 90% B for 9 min 54 s, the column was equilibrated at 3% B for 19 min 54 s. Eluted peptides were ionized in positive ion mode using a nanospray Flex with an electrospray ionization source (Thermo Fisher Scientific) and a fused-silica nano-bore emitter with an internal diameter of 10  $\mu$ m (New Objective, Woburn, MA, USA) at a capillary voltage of 1800 V. The ion

transfer tube temperature was set to 300 °C. Parent ion scans were carried out in the range 400–1300  $m/z$  in the Orbitrap mass analyzer at 120 K resolution with a maximum injection time of 120 ms and an AGC target value of  $2 \times 10^5$ . Data-dependent acquisition mode was set to top speed mode for precursor ion selection. The most intense peaks with (intensity threshold of  $5 \times 10^3$ ) were isolated with a quadrupole isolation width of 1.6  $m/z$ , fragmented by high-energy collisional dissociation (collision energy 30%) and detected in the ion-trap mass analyzer. A dynamic exclusion filter was applied for 30 s and excluded after one time. For ion-trap detection, the scan rate was set to a rapid scan range 400–1300  $m/z$ . The maximum injection time was 60 ms, and the AGC target value was  $1 \times 10^4$ .

### Protein identification by database matching

The LC–MS/MS data files were used to search the translated database of *F. metavorans* DSM105788 sequences (Additional file 2: FW16.IntegrationTable.xls) with Proteome Discoverer v2.0 (Thermo Fisher Scientific) including the search engine Sequest HT. The search parameters included precursor and product ion mass tolerances of 10 ppm and 0.5 Da, respectively, two missed cleavages allowed, cysteine carbamidomethylation as a fixed modification, and methionine oxidation as a variable modification. Proteins found with at least one unique peptide and a false discovery rate (FDR) of 1% (determined by percolator) were accepted [101].

### Enzymatic activity

Enzymatic hydrolysis was measured using the DNS method [102] after liquid fermentation at 50 °C for 24 or 96 h with the substrates arabinan, arabinoxytan, galactan, xylan, starch, CMC and polygalacturonic acid (all at 0.5%) or pectin citrus and laminarin (at 0.2%). We mixed 10  $\mu$ L of the *F. metavorans* extract with 50  $\mu$ L of each substrate and 40  $\mu$ L 50 mM citrate buffer (pH 4.8). Xylan was assayed for 10 min and the remaining substrates for 3 h. When *F. metavorans* was grown in YPD medium, we also measured CMC activity against CMC every 24 h for up to 7 days. Furthermore, if the fungus was cultivated in Mandels' mineral salts medium supplemented with 1% (w/v) cellulose and artificial cellulose substrates Avicel PH-101,  $\alpha$ -cellulose, HEC, H-CMC, M-CMC or L-CMC, we also measured the CMC activity on day 3. The protein concentration was determined using the ROTI Nanoquant protein detection kit (Carl Roth, Karlsruhe, Germany) by adding 50  $\mu$ L of the supernatant to 200  $\mu$ L of the detection solution. Measurements were collected from at least three experimental replicates.



### Saccharification of sugarcane bagasse and maize leaves

The conversion of 5% (w/v) NSCB, XSCB [44] and MZ into glucose, was tested in saturation curve assays supplemented with increasing amounts of the *F. metavorans* in-house crude enzymatic cocktail to a fixed amount of Accellerase 1500 (Genecor, Rochester, NY, USA) at final total cellulase activity of 5 FPU/g biomass, corresponding to 118 µg/mL. For the in-house enzymatic cocktail, the lyophilized secretome fractions from both biomass substrates were resuspended in 50 mM citrate buffer (pH 4.8) and combined at a 1:1 ratio (NSCB:MZ) before saturation curve experiments, such that the final protein concentration of  $312 \pm 2.7$  µg/mL represented 100%. Saccharification was carried out in 2-mL Eppendorf tubes containing 50 mM citrate buffer (pH 4.5) and up to 70% (v/v) of the in-house enzymatic cocktail from *F. metavorans* at 50 °C for 24 h in a thermomixer (Eppendorf, Hamburg, Germany) at an agitation rate of 1000 rpm. The amount of protein applied for the saturation curve experiments can be found in Additional file 1: Table S5. Each experiment was replicated and the reducing sugars were measured in triplicate using the DNS assay [102]. Glucose standards were used to calibrate the glucose released under each condition. The statistical significance (threshold  $p < 0.05$ ) was determined using Perseus ([www.coxdocs.org/doku.php](http://www.coxdocs.org/doku.php)).

### Supplementary Information

The online version contains supplementary material available at <https://doi.org/10.1186/s13068-021-01927-9>.

**Additional file 1: Figure S1:** Genomic DNA from *Fusarium metavorans* FW16.1 (DSM105788) was isolated using the CTAB method and 5 µL was mixed with 6 × loading buffer (0.25% (w/v) xylene cyanol, 0.25% (w/v) bromophenol blue, 30% (v/v) glycerol) and separated by 0.8% (w/v) agarose gel electrophoresis in Tris–borate EDTA (TBE) buffer at 80 V for 60 min, with the GeneRuler 1 kb Plus DNA Ladder (Thermo Fisher Scientific) as a marker. The DNA was stained with 1% ethidium bromide for 15 min and observed on a UV transilluminator (SynGene Genius, Biolmaging System). **Figure S2:** Specific CMCase activity of the supernatants against high-viscosity CMC over time in YPD medium. **Figure S3:** Specific CMCase activity of the supernatants using different synthetic nutrient sources. **Figure S4:** Enzymatic activities for polygalacturonase (A), laminarinase (B), CMCase (C) and xylanase (D). **Table S1:** CMCase activity of 48 fungal strains. **Table S2:** CAZyme analysis of fungal isolate FW16.1 and other fungal species. The coding regions were compared with the CAZyme database (Cantarel et al. 2009; Lombard et al. 2014). **Table S3:** Proteins of the fungal isolate FW16.1 induced on different synthetic and artificial cellulose and biomass substrates (maize leaves (MZ) or sugar cane bagasse (SCB)). The proteins were separated by SDS-PAGE followed by in-gel tryptic digestion and LC–MS/MS. The accession number, description, coverage (%), number of peptides (# peptides), peptide-to-spectrum matches (# PSMs), molecular weight in kDa (MW [kDa]), the calculated isoelectric point (calc. pI), Score Sequest HT and number of Peptides Sequest HT (# Peptides Sequest HT) were compared with the automated translation of the genome of the fungal isolate *Fusarium metavorans* DSM105788. BLASTP annotations and cellular functions are also shown. **Table S4:** Functional prediction of the CAZymes found on different synthetic and artificial cellulose and biomass substrates. **Table S5:** Quantity of protein applied in the saturation curve experiments.

**Additional file 2:** Integration table of the fungus.

**Additional file 3:** The phylogenetic tree provided by Dr. Kerry O'Donnell.

**Additional file 4:** The phylogenetic tree including the FW16.1 strain.

### Acknowledgements

We thank Dr. Richard L. Hahnke, Dr. Tobias Stacke, Kerry O'Donnell and David M. Geiser for valuable discussion and support. We thank Frank Förster, who helped assessing assembly quality, construction of trees and “polishing” of PacBio reads. We thank Richard M. Twyman for proofreading this manuscript.

### Authors' contributions

SCB isolated the fungal DNA and carried out ITS-PCR, secretome analysis and SDS-PAGE. HB cultivated the fungi and conducted the BLAST analysis of the proteins. BE measured the activities of the supernatants. SJ and KM analyzed the ITS-28S, *TEF1* and *RPB2* and genomic data and generated the phylogenetic tree. AA and HS carried out mass spectrometric proteomics. MR analyzed the FW16.1 genome. CB, CW and WS supervised the project. MG organized the laboratory work, coordinated the participating institutions and evaluated the data. All authors read and approved the final manuscript.

### Funding

Open Access funding enabled and organized by Projekt DEAL. This work was funded by the German federal ministry BMBF under contract no. 03A0150B within the framework of Bioeconomy International 2014. Dr. Arslan Ali acknowledges a fellowship under the faculty development program of the International Center for the Chemical and Biological Sciences, University of Karachi. Dr. Hévila Brognaro acknowledges financial support from the Fundação Faculdade de Medicina (FFM, São Paulo/Brazil).

### Availability of data and materials

All data generated or analyzed during this study are either included in this published article or can be found in the Supplementary Material.

### Declarations

#### Ethics approval and consent to participate

Not applicable.

#### Consent for publication

Not applicable.

#### Competing interests

The authors declare no competing interests.

#### Author details

<sup>1</sup> Faculty of Mathematics, Computer Science and Natural Science, Department of Biology, Biozentrum Klein Flottbek, Molecular Phytopathology, University of Hamburg, Ohnhorststr. 18, 22609 Hamburg, Germany. <sup>2</sup> Department of Parasitology, Institute of Biomedical Sciences, University of São Paulo, Av. Prof. Lineu Prestes, 1374, São Paulo, CEP 05508-000, Brazil. <sup>3</sup> Institute of Biochemistry and Molecular Biology, University of Hamburg, Martin Luther King Platz 6, 20146 Hamburg, Germany. <sup>4</sup> Dr. Panjwani Center for Molecular Medicine and Drug Research, International Center for Chemical and Biological Sciences, University of Karachi, University Road, Karachi 75270, Pakistan. <sup>5</sup> Institute of Clinical Chemistry and Laboratory Medicine Diagnostic Center, Campus Research, Martinstr. 52, N27, 20246 Hamburg, Germany. <sup>6</sup> Fraunhofer Institute for Translational Medicine and Pharmacology ITMP, Department Screening-Port, Schnackenburgallee 114, 22525 Hamburg, Germany. <sup>7</sup> Department Biology and Chemistry, Algorithmic Bioinformatics, Justus Liebig University Giessen, Heinrich-Buff-Ring 58, 35392 Giessen, Germany. <sup>8</sup> Department Biology and Chemistry, Institute of Food Chemistry and Food Biotechnology, Justus Liebig University Giessen, Heinrich-Buff-Ring 17, 35392 Giessen, Germany.

Received: 17 November 2020 Accepted: 11 March 2021

Published online: 20 March 2021

## References

- Ragauskas AJ, Williams CK, Davison BH, Britovsek G, Cairney J, Eckert CA, Frederick WJ, Hallett JP, Leak DJ, Liotta CL, et al. The path forward for biofuels and biomaterials. *Science*. 2006;311:484–9.
- Serrano-Ruiz JC, Luque R, Sepulveda-Escribano A. Transformations of biomass-derived platform molecules: from high added-value chemicals to fuels via aqueous-phase processing. *Chem Soc Rev*. 2011;40:5266–81.
- Ahorsu R, Medina F, Constantí M. Significance and challenges of biomass as a suitable feedstock for bioenergy and biochemical production: a review. *Energies*. 2018;11(12):3366.
- Leff B, Ramankutty N, Foley JA. Geographic distribution of major crops across the world. *Global Biogeochem Cy*. 2004;18(1).
- Parent B, Leclere M, Lacube S, Semenov MA, Welcker C, Martre P, Tardieu F. Maize yields over Europe may increase in spite of climate change, with an appropriate use of the genetic variability of flowering time. *PNAS*. 2018;115(42):10642–7.
- Nascimento MS, Santana ALBD, Maranhão CA, Oliveira LS, Bieber L. Phenolic extractives and natural resistance of wood; 2013.
- Gilbert HJ. The biochemistry and structural biology of plant cell wall deconstruction. *Plant Physiol*. 2010;153(2):444–55.
- Cantrell SA, Dianese JC, Fell J, Gunde-Cimerman N, Zalar P. Unusual fungal niches. *Mycologia*. 2011;103(6):1161–74.
- Chundawat SPS, Beckham GT, Himmel ME, Dale BE. Deconstruction of lignocellulosic biomass to fuels and chemicals. *Annu Rev Chem Biomol*. 2011;2:121–45.
- Himmel ME, Ding SY, Johnson DK, Adney WS, Nimlos MR, Brady JW, Foust TD. Biomass recalcitrance: engineering plants and enzymes for biofuels production. *Science*. 2007;315(5813):804–7.
- Bajpai P. Chapter 2-Xylan: occurrence and structure. In: *Xylanolytic enzymes*. Amsterdam: Academic Press; 2014. pp. 9–18.
- Holtzapfel MT. Hemicelluloses. In: Caballero B, Finglas P, Trugo L, editors. *Encyclopedia of food sciences and nutrition* (Second Edition). Oxford: Academic Press; 2003. p. 3060–71.
- York WS, Vanhalbeek H, Darvill AG, Albersheim P. Structural analysis of xyloglucan oligosaccharides by <sup>1</sup>H-NMR spectroscopy and fast-atom-bombardment mass-spectrometry. *Carbohydr Polym*. 1990;200:9–31.
- dos Santos MA, Grenha A. Chapter Seven—polysaccharide nanoparticles for protein and peptide delivery: exploring less-known materials. In: Donev R, editor. *Advances in protein chemistry and structural biology*. vol. 98. Academic Press; 2015. pp. 223–261.
- Willför S, Sundberg K, Tenkanen M, Holmbom B. Spruce-derived mannans—a potential raw material for hydrocolloids and novel advanced natural materials. *Carbohydr Polym*. 2008;72(2):197–210.
- Mohnen D. Pectin structure and biosynthesis. *Curr Opin Plant Biol*. 2008;11(3):266–77.
- Kashyap DR, Vohra PK, Chopra S, Tewari R. Applications of pectinases in the commercial sector: a review. *Bioresour Technol*. 2001;77(3):215–27.
- Dekker RFH. Biodegradation of the Hemicelluloses. In: Higuchi T, editor. *Biosynthesis and biodegradation of wood components*. Academic Press; 1985; pp. 505–533.
- Bonnin E, Pelloux J. Pectin degrading enzymes. In: Kontogiorgos V, editor. *Pectin: technological and physiological properties*. Cham: Springer International Publishing; 2020. p. 37–60.
- Chandel AK, da Silva SS, Singh OV. Detoxification of lignocellulose hydrolysates: biochemical and metabolic engineering toward white biotechnology. *Bioenerg Res*. 2013;6(1):388–401.
- Foston M, Ragauskas A. Biomass characterization: recent progress in understanding biomass recalcitrance. *Ind Biotechnol*. 2012;8:191–208.
- Meng XZ, Ragauskas AJ. Recent advances in understanding the role of cellulose accessibility in enzymatic hydrolysis of lignocellulosic substrates. *Curr Opin Biotech*. 2014;27:150–8.
- Sticklen MB. Plant genetic engineering for biofuel production: towards affordable cellulosic ethanol. *Nat Rev Genet*. 2008;9(6):433–43.
- de Souza AP, Leite DCC, Pattathil S, Hahn MG, Buckeridge MS. Composition and structure of sugarcane cell wall polysaccharides: implications for second-generation bioethanol production. *Bioenerg Res*. 2013;6(2):564–79.
- Meineke T, Manisseri C, Voigt CA. Phylogeny in defining model plants for lignocellulosic ethanol production: a comparative study of *Brachypodium distachyon*, wheat, maize, and *Miscanthus x giganteus* leaf and stem biomass. *PLoS ONE*. 2014;9(8):e103580.
- Yin YB, Mao XZ, Yang JC, Chen X, Mao FL, Xu Y. dbCAN: a web resource for automated carbohydrate-active enzyme annotation. *Nucleic Acids Res*. 2012;40(W1):W445–51.
- Lopes AM, Ferreira EX, Moreira LRS. An update on enzymatic cocktails for lignocellulose breakdown. *J Appl Microbiol*. 2018;125(3):632–45.
- Mueller GM, Bills GF. Introduction. In: *Biodiversity of fungi*. Burlington: Academic Press. 2004; pp. 1–4.
- Blackwell M. The fungi: 1, 2, 3, ... 5.1 million species? *Am J Bot*. 2011;98(3):426–38.
- Kirk PM, Cannon PF, Minter DW, Stalpers JA. *Dictionary of the fungi*, vol. 10. Wallingford, UK: CABI; 2008.
- O'Donnell K, Rooney AP, Proctor RH, Brown DW, McCormick SP, Ward TJ, Frandsen RJN, Lysøe E, Rehner SA, Aoki T, et al. Phylogenetic analyses of RPB1 and RPB2 support a middle cretaceous origin for a clade comprising all agriculturally and medically important fusaria. *Fungal Genet Biol*. 2013;52:20–31.
- Nelson PE, Dignani MC, Anaissie EJ. Taxonomy, biology, and clinical aspects of *Fusarium* species. *Clin Microbiol Rev*. 1994;7(4):479–80.
- Wollenweber H, Reinking O. *Die Fusarien: Ihre Beschreibung, Schadwirkung und Bekämpfung*. Berlin: P. Parey; 1935.
- Snyder WC, Hansen HN. The species concept in *Fusarium* with reference to section martiella. *Am J Bot*. 1941;28(9):738–42.
- Summerell BA, Laurence MH, Liew ECY, Leslie JF. Biogeography and phylogeography of *Fusarium*: a review. *Fungal Divers*. 2010;44(1):3–13.
- Coleman JJ. The *Fusarium solani* species complex: ubiquitous pathogens of agricultural importance. *Mol Plant Pathol*. 2016;17(2):146–58.
- Al-Hatmi AMS, Hagen F, Menken SBJ, Meis JF, de Hoog GS. Global molecular epidemiology and genetic diversity of *Fusarium*, a significant emerging group of human opportunists from 1958 to 2015. *Emerg Microbes Infect* 2016;5.
- O'Donnell K, Al-Hatmi AMS, Aoki T, Brankovics B, Cano-Lira JF, Coleman JJ, de Hoog GS, Di Pietro A, Frandsen RJN, Geiser DM, et al. No to *Neocosmospora*: phylogenomic and practical reasons for continued inclusion of the *Fusarium solani* species complex in the genus *Fusarium*. *mSphere*. 2020;5(5):e00810-00820.
- Muhammed M, Anagnostou T, Desalermos A, Kourkoumpetis TK, Carneiro HA, Glavis-Bloom J, Coleman JJ, Mylonakis E. *Fusarium* infection report of 26 cases and review of 97 cases from the literature. *Medicine*. 2013;92(6):305–16.
- Leslie JF, Summerell BA. *The Fusarium laboratory manual*. Ames, Iowa, USA: Blackwell Publishing; 2006.
- Coleman JJ, Rounsley SD, Rodriguez-Carres M, Kuo A, Wasmann CC, Grimwood J, Schmutz J, Taga M, White GJ, Zhou SG, et al. The genome of *Nectria haematococca*: contribution of supernumerary chromosomes to gene expansion. *Plos Genet*. 2009;5(8):e1000618.
- Kim JA, Jeon J, Park SY, Kim KT, Choi K, Lee HJ, Kim Y, Yang HS, Yeo JH, Lee YH et al. Genome sequence of an endophytic fungus, *Fusarium solani* JS-169, which has antifungal activity. *Microbiol Resour Ann*. 2017; 5(42).
- Brandt SC, Ellinger B, van Nguyen T, Thi QD, Van Nguyen G, Baschien C, Yurkov A, Hahnke RL, Schafer W, Gand M. A unique fungal strain collection from Vietnam characterized for high performance degraders of bioecological important biopolymers and lipids. *PLoS ONE*. 2018;13(8):e0202695.
- Rocha GJM, Gonçalves AR, Oliveira BR, Olivares EG, Rossell CEV. Steam explosion pretreatment reproduction and alkaline delignification reactions performed on a pilot scale with sugarcane bagasse for bioethanol production. *Ind Crops Prod*. 2012;35(1):274–9.
- Bhatia Y, Mishra S, Bisaria VS. Microbial  $\beta$ -glucosidases: cloning, properties, and applications. *Crit Rev Biotechnol*. 2002;22(4):375–407.
- Singhania RR, Patel AK, Sukumaran RK, Larroche C, Pandey A. Role and significance of  $\beta$ -glucosidases in the hydrolysis of cellulose for bioethanol production. *Bioresour Technol*. 2013;127:500–7.
- Gao J, Wakarchuk W. Characterization of five  $\beta$ -glycoside hydrolases from *Cellulomonas fimi* ATCC 484. *J Bacteriol*. 2014;196(23):4103–10.
- Glass NL, Schmoll M, Cate JHD, Coradetti S. Plant cell wall deconstruction by ascomycete fungi. *Annu Rev Microbiol*. 2013;67:477–98.
- van den Brink J, de Vries RP. Fungal enzyme sets for plant polysaccharide degradation. *Appl Microbiol Biotechnol*. 2011;91(6):1477–92.

50. Bey M, Zhou SM, Poidevin L, Henrissat B, Coutinho PM, Berrin JG, Sigolot JC. Cello-oligosaccharide oxidation reveals differences between two lytic polysaccharide monoxygenases (Family GH61) from *Podospora anserina*. *Appl Environ Microb*. 2013;79(2):488–96.
51. Phillips CM, Beeson WT, Cate JH, Marletta MA. Cellobiose dehydrogenase and a copper-dependent polysaccharide monoxygenase potentiate cellulose degradation by *Neurospora crassa*. *ACS Chem Biol*. 2011;6(12):1399–406.
52. Konno N, Ishida T, Igarashi K, Fushinobu S, Habu N, Samejima M, Isogai A. Crystal structure of polysaccharide lyase family 20 endo- $\beta$ -1,4-glucuronan lyase from the filamentous fungus *Trichoderma reesei*. *Febs Lett*. 2009;583(8):1323–6.
53. Chen JY, Guo XN, Zhu M, Chen C, Li DC. Polysaccharide monoxygenase-catalyzed oxidation of cellulose to glucuronic acid-containing cello-oligosaccharides. *Biotechnol Biofuels* 2019;12.
54. Prado-Martinez M, Anzaldo-Hernández J, Becerra-Aguilar B, Palacios-Juarez H, Vargas-Radillo JD, Renteria-Urquiza M. Characterization of maize leaves and of sugarcane bagasse to elaborate a mixed cellulose pulp. *Madera Bosques*. 2012;18(3):37–51.
55. Attia M, Stepper J, Davies GJ, Brumer H. Functional and structural characterization of a potent GH74 endo-xyloglucanase from the soil saprophyte *Cellvibrio japonicus* unravels the first step of xyloglucan degradation. *Febs J*. 2016;283(9):1701–19.
56. Foumani M, Vuong TV, Master ER. Altered substrate specificity of the gluco-oligosaccharide oxidase from *Acremonium strictum*. *Biotechnol Bioeng*. 2011;108(10):2261–9.
57. Lo Leggio L, Simmons TJ, Poulsen JCN, Frandsen KEH, Hemsworth GR, Stringer MA, von Freiesleben P, Tovborg M, Johansen KS, De Maria L et al. Structure and boosting activity of a starch-degrading lytic polysaccharide monoxygenase. *Nat Commun*. 2015;6.
58. Vu VV, Beeson WT, Span EA, Farquhar ER, Marletta MA. A family of starch-active polysaccharide monoxygenases. *PNAS*. 2014;111(38):13822–7.
59. Poutanen K, Sundberg M, Korte H, Puls J. Deacetylation of xylans by acetyl esterases of *Trichoderma reesei*. *Appl Microbiol Biot*. 1990;33(5):506–10.
60. Saykhedkar S, Ray A, Ayoubi-Canaan P, Hartson SD, Prade R, Mort AJ. A time course analysis of the extracellular proteome of *Aspergillus nidulans* growing on sorghum stover. *Biotechnol Biofuels* 2012;5.
61. Zhao ZT, Liu HQ, Wang CF, Xu JR. Comparative analysis of fungal genomes reveals different plant cell wall degrading capacity in fungi. *BMC Genomics*. 2013;14:274.
62. Borin GP, Sanchez CC, de Souza AP, de Santana ES, de Souza AT, Leme AFP, Squina FM, Buckeridge M, Goldman GH, Oliveira JVD. Comparative secretome analysis of *Trichoderma reesei* and *Aspergillus niger* during growth on sugarcane biomass. *PLoS ONE*. 2015;10(6):e0129275.
63. dos Santos HB, Bezerra TMS, Pradella JGC, Delabona P, Lima D, Gomes E, Hartson SD, Rogers J, Couger B, Prade R. *Myceliophthora thermophila* M77 utilizes hydrolytic and oxidative mechanisms to deconstruct biomass. *Amb Express*. 2016;6.
64. Couturier M, Navarro D, Favel A, Haon M, Lechat C, Lesage-Meessen L, Chevret D, Lombard V, Henrissat B, Berrin JG. Fungal secretomes of ascomycete fungi for biotechnological applications. *Mycosphere*. 2016;7(10):1546–53.
65. Benoit I, Coutinho PM, Schols HA, Gerlach JP, Henrissat B, de Vries RP. Degradation of different pectins by fungi: correlations and contrasts between the pectinolytic enzyme sets identified in genomes and the growth on pectins of different origin. *BMC Genomics*. 2012;13:321.
66. Lombard V, Ramulu HG, Drula E, Coutinho PM, Henrissat B. The carbohydrate-active enzymes database (CAZy) in 2013. *Nucleic Acids Res*. 2014;42(D1):D490–5.
67. Shradha SR, Sehgal S, Kamthania M, Kumar A. Laccase: microbial sources, production, purification, and potential biotechnological applications. *Enzyme Res*. 2011;2011:217861.
68. Obruca S, Marova I, Matouskova P, Haronikova A, Lichnova A. Production of lignocellulose-degrading enzymes employing *Fusarium solani* F-552. *Folia Microbiol*. 2012;57(3):221–7.
69. Scully ED, Hoover K, Carlson J, Tien M, Geib SM. Analysis of *Fusarium solani* isolated from the longhorned beetle, *Anoplophora glabripennis*. *PLoS ONE*. 2012;7(4):e32990.
70. Vuong TV, Foumani M, MacCormick B, Kwan R, Master ER. Direct comparison of glucooligosaccharide oxidase variants and glucose oxidase: substrate range and H<sub>2</sub>O<sub>2</sub> stability. *Sci Rep*. 2016;6.
71. Boraston AB, Bolam DN, Gilbert HJ, Davies GJ. Carbohydrate-binding modules: fine-tuning polysaccharide recognition. *Biochem J*. 2004;382:769–81.
72. Cantarel BL, Lombard V, Henrissat B. Complex carbohydrate utilization by the healthy human microbiome. *PLoS ONE*. 2012;7(6):e28742.
73. Seidl V, Huemer B, Seiboth B, Kubicek CP. A Complete survey of *Trichoderma* chitinases reveals three distinct subgroups of family 18 chitinases. *Febs J*. 2005;272(22):5923–39.
74. Schneider WD, Goncalves TA, Uchima CA, Couger MB, Prade R, Squina FM, Dillon AJP, Camassola M. *Penicillium echinulatum* secretome analysis reveals the fungi potential for degradation of lignocellulosic biomass. *Biotechnol Biofuels* 2016;9.
75. Machovič M, Janeček S. Domain evolution in the GH13 pullulanase subfamily with focus on the carbohydrate-binding module family 48. *Biologia*. 2008;63(6):1057–68.
76. Rocha VAL, Maeda RN, Pereira N, Kern MF, Elias L, Simister R, Steele-King C, Gomez LD, McQueen-Mason SJ. Characterization of the cellulolytic secretome of *Trichoderma harzianum* during growth on sugarcane bagasse and analysis of the activity boosting effects of swollenin. *Biotechnol Progr*. 2016;32(2):327–36.
77. Marx IJ, van Wyk N, Smit S, Jacobson D, Viljoen-Bloom M, Volschenk H. Comparative secretome analysis of *Trichoderma asperellum* S4F8 and *Trichoderma reesei* rut C30 during solid-state fermentation on sugarcane bagasse. *Biotechnol Biofuels*. 2013;6(1):172.
78. Delabona PD, Cota J, Hoffmam ZB, Paixão DAA, Farinas CS, Cairo JPLF, Lima DJ, Squina FM, Ruller R, Pradella JGD. Understanding the cellulolytic system of *Trichoderma harzianum* P49P11 and enhancing saccharification of pretreated sugarcane bagasse by supplementation with pectinase and  $\alpha$ -L-arabinofuranosidase. *Bioresour Technol*. 2013;131:500–7.
79. Rodriguez A, Perestelo F, Carnicero A, Regalado V, Perez R, de la Fuente G, Falcon MA. Degradation of natural lignins and lignocellulosic substrates by soil-inhabiting fungi imperfecti. *Fems Microbiol Ecol*. 1996;21(3):213–9.
80. Mitra J, Mukherjee PK, Kale SP, Murthy NBK. Bioremediation of DDT in soil by genetically improved strains of soil fungus *Fusarium solani*. *Biodegradation*. 2001;12(4):235–45.
81. Wang K, Chen J, Sun S-N, Sun R-C. Chapter 6 - Steam Explosion. In: Pandey A, Negi S, Binod P, Larroche C, editors. *Pretreatment of biomass*. Amsterdam: Elsevier; 2015. p. 75–104.
82. Anwar Z, Gulfranz M, Irshad M. Agro-industrial lignocellulosic biomass a key to unlock the future bio-energy: a brief review. *J Radiat Res Appl Sci*. 2014;7(2):163–73.
83. Sindhu R, Binod P, Pandey A. Biological pretreatment of lignocellulosic biomass—an overview. *Bioresour Technol*. 2016;199:76–82.
84. Sun SM, Sun SL, Cao XF, Sun RC. The role of pretreatment in improving the enzymatic hydrolysis of lignocellulosic materials. *Bioresour Technol*. 2016;199:49–58.
85. CSH Protocols: YPD media. *Cold Spring Harb Protoc* 2010, 2010(9):pdb.rec12315.
86. Leach J, Lang BR, Yoder OC. Methods for selection of mutants and in vitro culture of *Cochliobolus heterostrophus*. *J Gen Microbiol*. 1982;128:1719–29.
87. Raper KB, Thom C. *A manual of the penicillia*. Baltimore: Williams and Wilkins; 1949.
88. Mohseni M, Norouzi H, Hamed J, Roohi A. Screening of antibacterial producing actinomycetes from sediments of the Caspian Sea. *Int J Mol Cell Med*. 2013;2(2):64–71.
89. Mandels M, Reese ET. Induction of cellulase in fungi by cellobiose. *J Bacteriol*. 1960;79(6):816–26.
90. Doyle JJ, Doyle JL. Isolation of plant DNA from fresh tissue. *Focus*. 1990;12:13–5.
91. Richards E, Reichardt M, Rogers S. Preparation of genomic DNA from plant tissue. *Current protocols in molecular biology* 1994, Chapter 2.
92. White TJ, Bruns T, Lee S, Taylor J. Amplification and direct sequencing of fungal ribosomal RNA genes for phylogenetics. In: Innis M, Gelfand D, Sninsky J, White T, editors. *PCR protocols: a guide to methods and applications*. Orlando, Florida: Academic Press; 1990. p. 315–22.

93. Brankovics B, Zhang H, van Diepeningen AD, van der Lee TAJ, Waalwijk C, de Hoog GS. GRAB: selective assembly of genomic regions, a new niche for genomic research. *Plos Comput Biol*. 2016;12(6):e1004753.
94. Ye YZ, Choi JH, Tang HX. RAPSearch: a fast protein similarity search tool for short reads. *BMC Bioinform* 2011;12.
95. Zhao YA, Tang HX, Ye YZ. RAPSearch2: a fast and memory-efficient protein similarity search tool for next-generation sequencing data. *Bioinformatics*. 2012;28(1):125–6.
96. Finn RD, Bateman A, Clements J, Coggill P, Eberhardt RY, Eddy SR, Heger A, Hetherington K, Holm L, Mistry J, et al. Pfam: the protein families database. *Nucleic Acids Res*. 2014;42(D1):D222–30.
97. Hahnke RL, Stackebrandt E, Meier-Kolthoff JP, Tindall BJ, Huang SX, Rohde M, Lapidus A, Han J, Trong S, Haynes M et al. High quality draft genome sequence of *Flavobacterium rivuli* type strain WB 3.3-2(T) (DSM 21788(T)), a valuable source of polysaccharide decomposing enzymes. *Stand Genomic Sci* 2015;10.
98. Zhang H, Yohe T, Huang L, Entwistle S, Wu PZ, Yang ZL, Busk PK, Xu Y, Yin YB. dbCAN2: a meta server for automated carbohydrate-active enzyme annotation. *Nucleic Acids Res*. 2018;46(W1):W95–101.
99. Mandels M, Weber J. The production of cellulases. *Am Chem Soc*. 1969;95:391.
100. Laemmli UK. Cleavage of structural proteins during the assembly of the head of bacteriophage T4. *Nature*. 1970;227:680.
101. Shevchenko A, Tomas H, Havlis J, Olsen JV, Mann M. In-gel digestion for mass spectrometric characterization of proteins and proteomes. *Nat Protoc*. 2007;1:2856–60.
102. Miller GL. Use of dinitrosalicylic acid reagent for determination of reducing sugar. *Anal Chem*. 1959;31:426.

### Publisher's Note

Springer Nature remains neutral with regard to jurisdictional claims in published maps and institutional affiliations.

Ready to submit your research? Choose BMC and benefit from:

- fast, convenient online submission
- thorough peer review by experienced researchers in your field
- rapid publication on acceptance
- support for research data, including large and complex data types
- gold Open Access which fosters wider collaboration and increased citations
- maximum visibility for your research: over 100M website views per year

At BMC, research is always in progress.

Learn more [biomedcentral.com/submissions](https://biomedcentral.com/submissions)

